LUT University

LUT School of Energy Systems

LUT Mechanical Engineering

Mengqi Wang

A Compact High-Power-Density Servo Drive Design

Examiner(s): Associate Professor Ph.D Huapeng Wu,

Post-doctoral Researcher Ph.D Ming Li

ABSTRACT

Brushless DC motors are indispensable components in contemporary industrial, medical, military and household appliances. Due to its high efficiency, long life, large starting torque and flexible control speed control, it has received extensive attention. With the rapid development of modern motor technology and communication technology, the size of heavy-duty industrial equipment, precision control instruments and advanced detection devices is reduced, and a compact brushless DC motor driver with high integration and reliability and advanced communication networks interface is compatible to meet the requirement of the market and industrial.

This thesis is investigating how to design and evaluate a compact drive module to drive three phase BLDC motor with both hardware and software for the brushless DC motor control system in a significant compact size, which could be used on medical equipment, robot arm and vehicles in a small scale. This research investigates the fundamental mathematical BLDC motor model and develops controllers and motor driver according to certain design requirements. The motor driver is designed based on the STM32F107 microcontroller from STMicroelectronics and the DRV8332 Integrated Digital Motor Control module with a three-stage power supply strategy. To achieve the correct commutation of the BLDC motor, three complementary PWM drive signals, motor control communication command and several warning structures have been built. Finally, a compact PCB board with corresponding driving program are presented with proved performance.

ACKNOWLEDGEMENTS

Mengqi Wang
10.06.2019

TABLE OF CONTENTS

LIST OF SYMBOLS AND ABBREVIATIONS

θ_e — The angle between the rotor and the coordinate axis [rad]

ω_r — Rotor angular velocity [rad/s]

C_{over} — The overflow counter

$Current\_s$ — Current feedback signal

$e_a, e_b \ e_c$ — Phase back EMFs [V]

$f_{sampling}$ — Sampling frequency of the Hall signal [Hz]

$i_a \ i_b \ i_{c,}$ — Phase currents of the motor [A]

k_e — Back EMF coefficient of the motor

$L_a \ L_b \ L_{c,}$ — Phase self-equivalent inductances of the motor [H]

$M_a \ M_b \ M_c$ — Phase mutual inductances of the motor [H]

$P_A \ P_B \ P_C$ — The power loss on each phase of the motor [W]

P_{ins} — The instantaneous power [W]

P_t — The total power lose of the motor [W]

$R_a, R_b, R_{c,}$ — Phase equivalent resistances of the motor [Ω]

$Speed\_s$ — Speed feedback signal

T_e — Electromagnetic torque [kg·m^2·s^{-2}]

T_{pulse} — The period of one pulse of TIM4 of STM32F107 [s]

$U_a \ U_b \ U_c$ — The motor terminal voltage [V]

U_i — Input voltage of control system [V]

U_n — Motor neutral point voltage [V]

V — The rotate speed of motor [rpm]

V_{out} — output voltage across the sampling resistor [V]

V_{REF} — Reference voltage [V]

V_{SENSE} — Detection voltage of the sampling resistor [V]

ADC — Analog-to-digital

$BLDC$ — Brushless Direct Current

CAN — Controller Area Network

DMA — Direct Memory Access

DSP — Digital Signal Processing

EMF — Electromotive force

GND	Electronical ground
GTO	Gate turn-off thyristor
GVDD	Gate-drive voltage supply
I2C	Inter-Integrated Circuit
IEGT	Injection Enhanced Gate Transistor
IGCT	integrated gate-commutated thyristor
JTEG	Joint Technology Exchange Group
LQFP	Low Profile Quad Flat Pack
MAC	media access control
MCU	microcontroller unit
MOSFET	metal–oxide–semiconductor field-effect transistor
OTW	Overtemperature warning
PCB	Printed Circuit Board
PID	proportional–integral–derivative
PMSM	Permanent Magnet Synchronous Motor
PVDD	Power supply input for half-bridge
PWM	Pulse-Width Modulation
SPI	Serial Peripheral Interface
SRAM	Static random-access memory
UART	Universal asynchronous receiver-transmitter

1 INTRODUCTION

1.1 Background

Brushless DC motors are widely used in electric vehicles, industrial robots, advanced CNC machine tools, medical equipment and home appliances due to their output torque, good speed regulation and high operating efficiency. High-performance drivers with versatility, high integration and integrated intelligent control algorithms are the current trends in the motor driver products development process. The cost of designing, manufacturing and maintaining advanced control systems are reduced due to the widespread adoption and application of electronic products and microcontrollers in modern industries. Therefore, it is meaningful to develop a compact brushless motor drive type with high efficiency, high power density, suitable for control equipment and relatively low-cost automation equipment [1-3].

Currently, the development of brushless DC motors is the most appreciate technology program in the motor industry. The R&D objectives are in a wide range of motor design optimization, winding technology improvement, electromagnetic material improvement of steel sheet, magnetic field characteristic enhancement and advanced sophisticated electronic control technology. The industry, government and academia are integrated together to enhance relative technologies and core components such as integrated and matching technologies, system build and drive control [4].

As a result of wide application of BLDC motors, more compact and efficient drive equipment needs to be designed. Tze-Yee Ho[5] presents a design of implement of an electric foot rehabilitation machine which is based on a brushless DC motor drive. This device is to help patients who need physical therapy for a foot. If it is promoted in the application, a more compact design is needed. B. Abdi designed a simple analog BLDC drive control system for electro-mechanical energy storage system which can be used in Low Earth Orbit (LEO) satellites to improve the energy storage system by transferring electrical energy to rotational kinetic energy and stored in a flywheel with a high speed[6-7]. As a device which is used in the aerospace field, volume and quality needed to be optimized. Be-sides, the small scale and size motors are widely applied in visual equipment such as computer disc drives, tape recorders and digital audio device [8] and Modern civilian equipment will be more intelligent and miniaturized with the ad-vancement of electronic technology. The cost

of controllers for BLDC motors is needed to reduce and many schemes with advanced algorithms for reduced cost controllers have been reported in the literature[9-10] with two primary technolo-gies: topological approach and control approach to optimize the performance from both algorithms and hardware devices such as switches, sensors and asso-ciated circuit.

1.2   Main Work of the thesis

The motivation of this thesis is to design and evaluate a compact drive module to drive three phase BLDC motor with both hardware and software for the brushless DC motor control system in a significant compact size, which could be used in medical equipment, robot arm and vehicles with a small scale.

To achieve the research goal, the follow tasks should be done:

1. Study the fundamental of the BLDC motor
2. Analyze the operation condition of BLDC motor
3. Develop a motor drive platform including motor control and feedback system
4. Develop the corresponding software on ARM micro-controller
5. Prove the performance of the device and write conclusion

In this research, the following technical innovations are made:

1. A hardware scheme of three phase brushless DC motor with Hall sensor interface and current feedback interface are developed
2. Three stages voltage regulator circuit is designed
3. The program of PWM wave generator, motor synchronization signal processing, control instructs and current detection on an ARM framework is delivered
4. Recommendations of developing motor drive of both hardware and software are carried out

A three phase Brushless DC motor drive scheme both of hardware and software have been built. The practical significance lies in the fact that the analysis of the operation principle of BLDC motor allows us to model and evaluate the effective design of a compact motor drive, based on circuit principle and analysis, PCB design, embedded system programming, control signal processing and software interface design. To apply a compact high-power density motor drive on industrial control, medical and aerospace could reduce space for related

mechanical design. Detailed and effective design solutions can provide a reference for future optimization.

1.3   Thesis Structure

The chapter 1 introduces the fundamental knowledge of BLDC motor both motor structure and mathematical model. The chapter 2 analyzes the requirement of de-veloping a BLDC motor drive. Hardware and software are designed at chapter 3 and chapter 4. The chapter 5 shows the result of the whole experiment and the chapter 6 conclude the developing process of this thesis. Other external materials are given by appendixes.

2   FUNDAMENTALS OF THE BUSHLESS DC MOTOR

2.1   Overview

Brushless DC motors must be equipped with an electronic controller for proper operation.

The primary function of the latter is to achieve electronic commutation of the windings. The overall structure of the brushless DC motor system is shown in the figure 1. It mainly consists of a BLDC motor, a motor driver, a controller and a feedback signal by sensors.
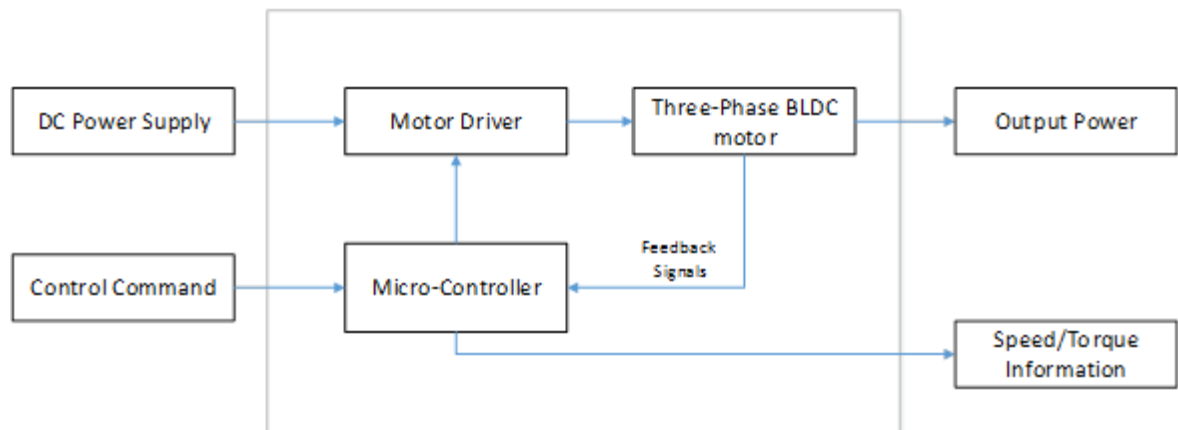
Figure 1. Brushless Motor System Structure.

2.2   Development of BLDC motor

To upgrade the commutator unit in the motor, in 1917, the Boliger used a rectifier tube instead of the brush element of the brushed DC motor, and the basic design concept of the brushless motor was established. Benefiting from the development of semiconductor technology and industry, Bell Labs successfully developed switching transistors in 1948; In 1955, D. Harrison from the United States applied for the first patent of transistor commutator instead of motor mechanical commutator, marking the birth of modern permanent magnet brushless DC motor. However, this brushless motor had serious defects that could not be self-started, and the power consumption of the transistor switch was too large. In 1962, after the reversing permanent magnet brushless motor that achieved position detection through Hall elements was invented, the development of brushless motors began to be paid attention to.

After the 1970s, with the rapid development of power electronic switching devices and the invention of various advanced position sensors, such as proximity switches position sensors, electromagnetic resonance position sensors, high-frequency coupled position sensors and photoelectric position sensors, magnetic brushless DC motors have achieved long-term development[11-13].

2.2.1 Motor body

The brushless DC motor is basically the same as the brushed DC motor in the electromagnetic structure, but its armature winding is placed on the stator. The weight of the rotor is used, the structure is simplified, the performance is im-proved, and the reliability is improved.

Unlike a brushed DC motor, the stator winding of a brushless DC motor acts as an armature, and the field winding is replaced by a permanent magnet material. According to the current waveform flowing into the armature winding, the DC brushless motor can be divided into a square wave DC motor (BLDC motor) and a sine wave DC motor. The BLDC motor replaces the mechanical commuta-tion of the original DC motor by electronic commutation[14].

The permanent magnet material is used as the rotor, eliminating the need for brushes; while the PMSM replaces the field windings in the rotor of the synchro-nous motor with permanent magnet materials, eliminating the excitation wind-ings, slip rings and brushes. Under the same conditions, it is easier to obtain a square wave in the driver circuit, and the control is simple. Therefore, the application of BLDCM is much wider than that of PMSM.

The development of brushless motors is inseparable from the development of permanent magnet materials. The development of magnetic materials has basical-ly gone through the following stages of development: AlNiCo, ferrite magnetic materials, NdFeB. NdFeB has a high magnetic energy product, and its appear-ance has caused a revolution in magnetic materials. The application of the third generation NdFeB permanent magnet material further reduces the amount of copper used in the motor and promotes the development of brushless motors in the direction of high efficiency, miniaturization and energy saving[15].

2.2.2 Control Algorithm

In modern industry, the requirements for motor performance are getting higher and higher, and the improvement of motor performance is mainly through the following two ways: First, the research on the motor body is mainly to adopt special structure to improve the performance of the motor; the other way is to adopt advanced control strategy. Experts from various countries are studying the application of modern control theory and intelligent control theory to brushless DC motor control, such as direct torque control, neural network control, fuzzy control, variable structure, robust regulator, parameter adaptive control and other advanced control[16-17].

It is difficult to achieve high control requirements by only using classical PID control. It is inevitable that there will be shortcomings such as large overshoot and slow response time. However, if the modern control theory is applied to the design, the calculation amount is often very large, and it is difficult to realize real-time control.

With the development of high-performance DSP and other control devices, the cost performance is continuously improved, and the computational complexity is solved to a certain extent, which makes the modern control theory and intelligent control theory further applied, and the control performance of the motor is further improved[18].

2.2.3 Drive Circuit

At present, the control circuit generally has three forms of an application specific integrated circuit, a microprocessor and a digital signal processor.

In the case where the motor control requirements are not high, the control circuit composed of professional integrated circuits is a simple and practical method; since the digital signal processor has fast operation and few peripheral circuits, the system composition can be made in a compact size.

The drive circuit outputs electrical power that drives the armature windings of the motor and is controlled by the control circuit. The drive circuit consists of high-power switching devices. It is precisely because of the emergence of thyris-tors that DC motors have evolved from brushed to brushless. However, since the thyristor is a semi-controlled switching device

with only control switching and no self-shutdown capability, its switching frequency is low, which cannot satisfy the further improvement of the performance of the brushless DC motor. With the rapid development of power electronics technology, there are fully-controlled power switching devices, including turn-off transistors (GTO), power field effect transistors (MOSFETs), metal gate bipolar transistor IGBT modules, and inte-grated gate switching. Flow thyristor (IGCT) and newly developed electron injection enhancement gate transistor (IEGT) [15].

At present, the full-control switching device is gradually replacing the ordinary thyristor with complicated circuit, large volume and low function index. The driving circuit has been switched from the linear amplification state to the pulse width modulation switching state, and the corresponding circuit composition is also transferred from the power tube discrete circuit. As a modular integrated cir-cuit, it creates conditions for intelligent, high-frequency and miniaturization of the drive circuit.

2.3   BLDC Motor Structure

Unlike the brushed DC motor design concept, the brushless DC motor initially interchanges the stator and rotor positions of the DC motor, making the rotor a permanent magnet structure.

The permanent magnet structure also becomes a permanent magnet steel, which is composed of a certain number of pole pairs and has an arc shape. There is a uniform air gap beside the magnetic pole of the rotor, and the magnetic flux density of the air gap is trapezoid ally distributed to obtain the air gap flux.

The stator is an armature winding, and the stator three-phase winding is generally a concentrated winding. Rare earth materials are widely used in magnetic steel to produce high residual flux density and large coercive force. In addition, the rare earth permanent magnet material has a large magnetic resistance to the radial axis of the motor and the magnetic field of the straight axis. Because the magnetic permeability is, like the magnetic permeability of air, the armature reaction can be minimized [15,19].

With the practical application of the new permanent magnet material NdFeB, the rotor structure of the motor has more diverse developments, such as disc structure and outer rotor structure, high torque, high precision, miniaturization and environmental resistance are applied in order to develop trends and in a wider field. As is shown in the figure 2.
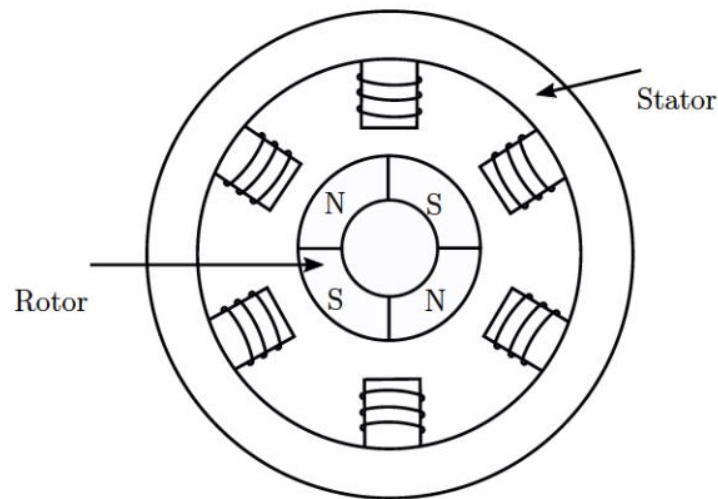
Figure 2. Fundamental BLDC Motor Structure.

Brushless motor is driven by Square wave current drive. The common three-phase bridge type 6-state operation mode in one electrical cycle time of 360° direction is divided into six sections, which are used to indicate six states where the three-phase windings are turned on. The A, B, C of the three-phase winding ends are connected to the three bridge arms of a three-phase bridge inverter composed of six high-power switching devices. When the winding is in the Y solution, two of the six states have two windings connected in series and one is intended to be forward conduction, one is in a reverse conduction. Another winding end corresponds to the upper and lower bridges are not conductive. As is shown in the Fig. 3.
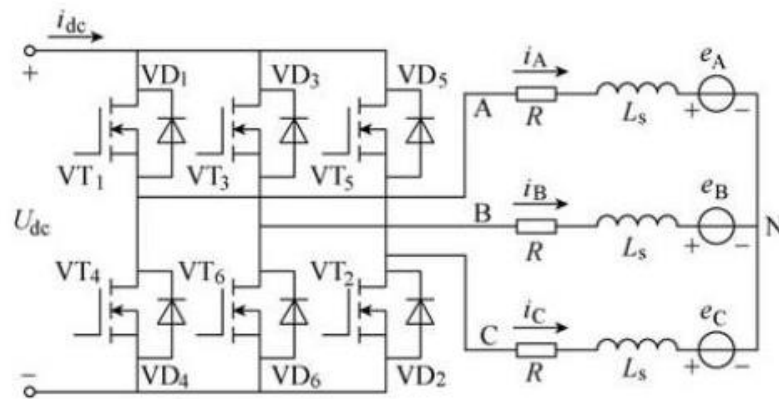
Figure 3. Three-phase bridge inverter circuit of brushless DC motor.

2.4   Sensored and Sensorless Feedback System

According to the working principle of the three-phase brushless DC motor, the driver needs to generate a square wave signal to drive the motor. Sensored and Sensorless feedback control are the two main synchronous driving methods of brushless DC motors. As is shown in the figure.4.
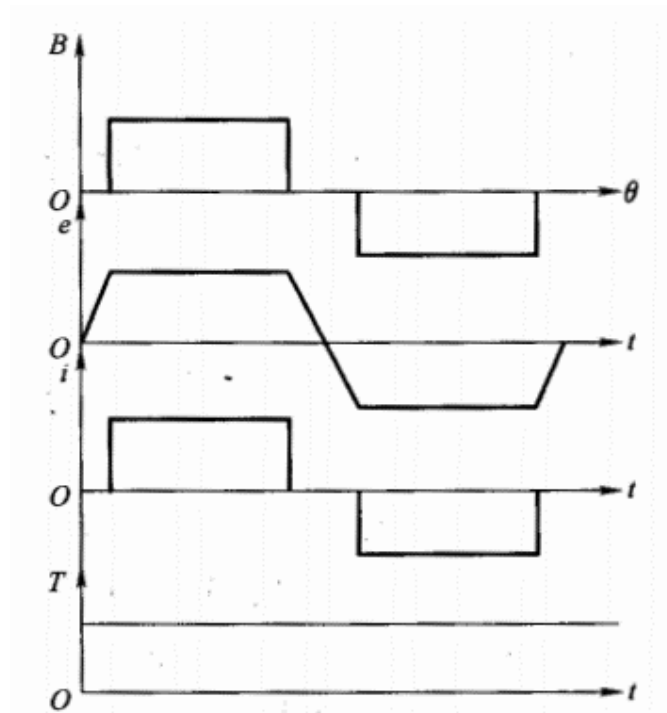
Figure 4. The flux density distribution, back electromotive force, phase current and electromagnetic torque of the BLDC motor driven by the wave under ideal conditions.

2.4.1 Sensorless Control

Sensorless brushless DC motors do not have built-in sensors. Its working principle is to drive the motor synchronisation is driven by detecting the signal of the counter electromotive force zero crossing generated by the motor. Besides, since the frequency generated by the back electromotive force is proportional to the speed of the motor, the speed of the motor can be determined by reading these frequencies and the corresponding drive mode adjustment can be made. As is shown in the figure 5.
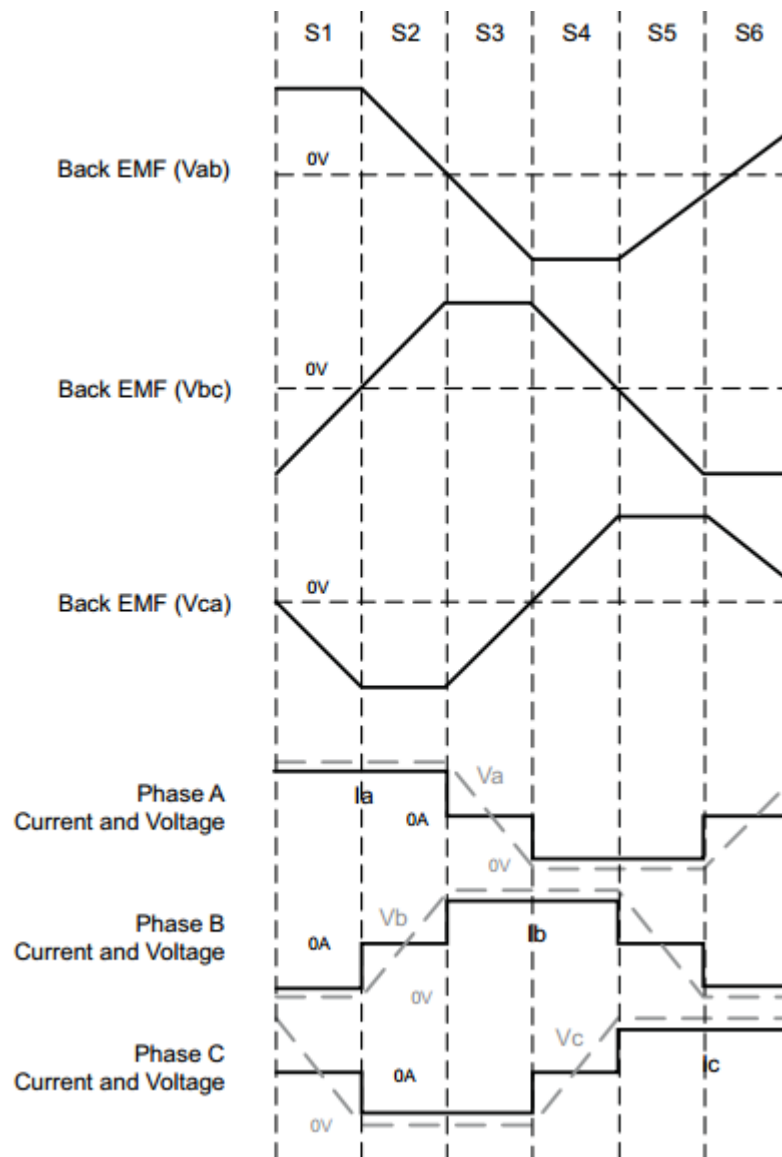
Figure 5. Sensorless Control Scheme.

A key drawback of this approach is that the back EMF at very low speed is very weak, making it difficult to obtain reliable and stable data. Simultaneously starting a sensorless BLDC motor can also be a problem.

2.4.2 Sensored Control

Sensored BLDC motors are usually equipped with position sensors which is the same as Hall effect sensors that come with motor. These position sensors are evenly mounted inside the motor at a fixed angle towards each other. Normally, brushless motor with Hall elements has three Hall sensors distributed with a difference of 120°. In the running process of the motor, the rotor position of the motor is determined by the magnetic field transformation of the stator and the rotor, and its status is fed back to the controller through a Boolean signal.

The main advantage of this type of motors is the ability to create a closed loop control system and to determine the position of the rotor to improve control accuracy. In addition, by detecting the speed at which the Hall signal changes, the rotational speed of the motor can be determined. Its disadvantage is that it relies too much on the sensor's feedback signal. Under some extreme environments, for instance dust, vibration, humidity may give rise to a sensor failure.

2.5   Mathematical Model of BLDC Motor

Figure 6. is an analysis of three phase windings BLDC motor with Y connection.
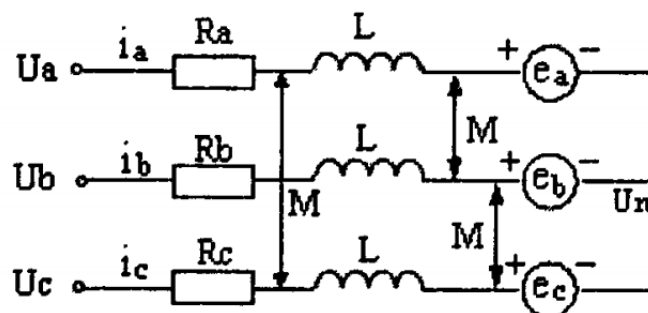
Figure 6. Equivalent circuit diagram of BLDC motor.

To simplify the analysis, make the following assumptions:

- The stator windings are spaced 60° apart
- Do not consider cogging and magnetic saturation
- Three-phase stator winding symmetry, $R_a = R_b = R_c$, $L_a = L_b = L_c$, $M_a = M_b = M_c$
- Ignore the influence of physical factors such as temperature, hysteresis and eddy current on parameters

2.5.1 Voltage equation of brushless DC motor

According to figure 6, the voltage balance equation of the motor is:

$$\begin{bmatrix} U_a - U_n \\ U_b - U_n \\ U_c - U_n \end{bmatrix} = \begin{bmatrix} R & 0 & 0 \\ 0 & R & 0 \\ 0 & 0 & R \end{bmatrix}\begin{bmatrix} i_a \\ i_b \\ i_c \end{bmatrix} + \begin{bmatrix} L & M & M \\ M & L & M \\ M & M & L \end{bmatrix}\begin{bmatrix} \dfrac{di_a}{dt} \\ \dfrac{di_b}{dt} \\ \dfrac{di_c}{dt} \end{bmatrix} + \begin{bmatrix} e_a \\ e_b \\ e_c \end{bmatrix} \quad (1)$$

Where,

Ua, Ub, Uc - the motor terminal voltage in V;

Un - motor neutral point voltage in V;

ia, ib, ic - the phase currents in A;

ea, eb, ec - the phase back EMFs in V;

R - the phase stator resistance that is same for three phases in Ω;

L - the self-inductances in H;

M - the mutual inductances in H

Due to Y connection, $i_a + i_b + i_c = 0$. and $M\,i_a + M i_b + M\,i_c = 0$. Therefore, the form X.Y could be transfer to:

$$\begin{bmatrix} U_a - U_n \\ U_b - U_n \\ U_c - U_n \end{bmatrix} = \begin{bmatrix} R & 0 & 0 \\ 0 & R & 0 \\ 0 & 0 & R \end{bmatrix}\begin{bmatrix} i_a \\ i_b \\ i_c \end{bmatrix} + \begin{bmatrix} L - M & 0 & 0 \\ 0 & L - M & 0 \\ 0 & 0 & L - M \end{bmatrix}\begin{bmatrix} \dfrac{di_a}{dt} \\ \dfrac{di_b}{dt} \\ \dfrac{di_c}{dt} \end{bmatrix} + \begin{bmatrix} e_a \\ e_b \\ e_c \end{bmatrix} \quad (2)$$

Let $L' = L - M$ be the equivalent inductance of the stator windings of each phase of the motor, then equation:

$$\begin{bmatrix} U_a - U_n \\ U_b - U_n \\ U_c - U_n \end{bmatrix} = \begin{bmatrix} R & 0 & 0 \\ 0 & R & 0 \\ 0 & 0 & R \end{bmatrix} \begin{bmatrix} i_a \\ i_b \\ i_c \end{bmatrix} + \begin{bmatrix} L' & 0 & 0 \\ 0 & L' & 0 \\ 0 & 0 & L' \end{bmatrix} \begin{bmatrix} \dfrac{di_a}{dt} \\[2mm] \dfrac{di_b}{dt} \\[2mm] \dfrac{di_c}{dt} \end{bmatrix} + \begin{bmatrix} e_a \\ e_b \\ e_c \end{bmatrix} (3)$$

The phase voltages U_A, U_B, U_C of motor could be written as:

$$\begin{bmatrix} U_A \\ U_B \\ U_C \end{bmatrix} = \begin{bmatrix} U_a - U_n \\ U_b - U_n \\ U_c - U_n \end{bmatrix} (4)$$

When the motor is working during non-phase-changing period, assume i and j phases are connected (i, j = a, b, c, and i ≠ j). Combined with equations (3) and (4) can be obtained:

$$U_n = \frac{U_i - U_j}{2} - \frac{e_i - e_j}{2} (5)$$

When the motor is working during phase-changing period, it can be obtained:

$$U_n = \frac{U_A + U_B + U_C}{3} - \frac{e_a + e_b + e_c}{2} (6)$$

2.5.2 Back EMFs

The back EMF waveform of the brushless DC motor is a trapezoidal wave as shown in Figure 7. It is the relationship between EMFs and motor phase current.
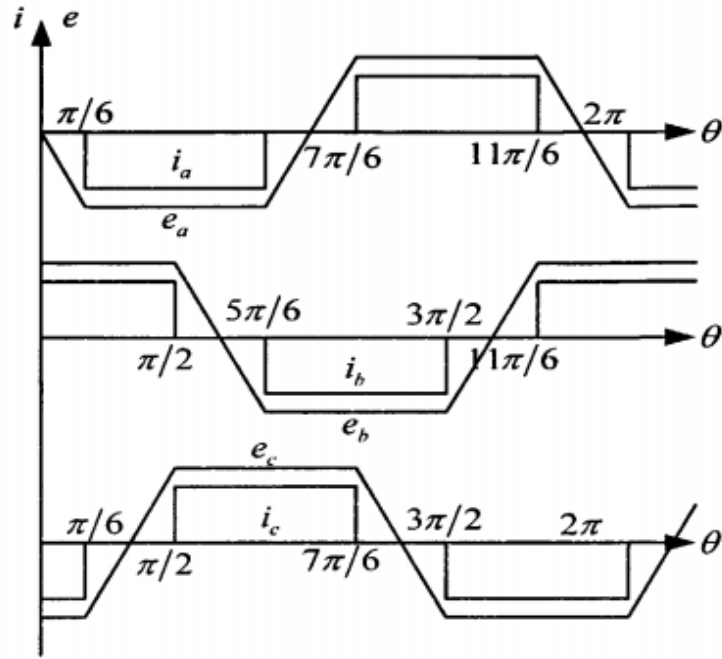
Figure 7. Back EMFs waveform with phase currents.

It can write the expression of *e* according to the piecewise function equation taking e$_a$ as an example:

$$
e_a = \begin{cases}
-k_e\omega_r \times \dfrac{\theta_e}{\frac{\pi}{6}} & 0 \leq \theta_e \leq \pi/6 \\
-k_e\omega_r\pi/6 \leq \theta_e \leq 5\pi/6 \\
-k_e\omega_r \times \dfrac{\theta_e - \pi}{\frac{\pi}{6}} & 5\pi/6 \leq \theta_e \leq 7\pi/6 \\
k_e\omega_r 7\pi/6 \leq \theta_e \leq 11\pi/6 \\
k_e\omega_r \times \dfrac{2\pi - \theta_e}{\frac{\pi}{6}} & 11\pi/6 \leq \theta_e \leq 2\pi
\end{cases} \quad (7)
$$

Where,

k_e - back EMF coefficient of the motor;

ω_r - rotor angular velocity in rad/s;

θ_e - the angle between the rotor and the coordinate axis a in rad.

e$_b$ and e$_c$ lag 120° and 240° angles, respectively.

2.5.3 Electromagnetic Torque

Each phase of the brushless motor consists of an equivalent resistor and an equivalent inductor. The stator current flowing through the windings of each phase creates a magnetic field to store energy while losing. When phase currents flow through back-EMF sources, the instantaneous power P_{inst} absorbed by sources can be derived as[15, 20]:

$$P_{ins} = e_a i_a + e_b i_b + e_c i_c \ (8)$$

Converting this power into mechanical power gives electromagnetic torque:

$$T_e = \frac{P_{ins}}{\omega} = (e_a i_a + e_b i_b + e_c i_c)/\omega \ (9)$$

Because back-EMFs are proportional to speed, the electromagnetic torque can be given as:

$$T_e = K_t[f_a(\theta_r)i_a + f_b(\theta_r)i_b + f_c(\theta_r)i_c] = K_t(2I_{pd}) \ (10)$$

Where,

K_t - torque constant;

I_{pd} - the peak value of the phase current in A.

2.5.4 Equation of motion for brushless DC motor

If the viscous friction and torsional elasticity in the transmission mechanism of the electric drive system are neglected, the equation of motion of the brushless DC motor system is:

$$T_e - T_L = J\frac{d\Omega}{dt} = \frac{J}{p}\frac{d\omega}{dt} \ (11)$$

Where,

T_e is electromagnetic torque;

T_L is load torque;

J is motor moment of inertia;

Ω is mechanical angular velocity of motor;

p is number of pole pairs

ω is electric angular velocity of the motor.

The relationship among the position angle of the rotor θ_e, ω, Ω is:

$$\frac{d\theta_e}{dt} = \omega = p\Omega \ (12)$$

For brushless DC motors, the relationship among speed n (rpm), pole pair p and supply frequency f (Hz)is:

$$n = \frac{60f}{p} \ (13)$$

2.6 Summarize

This section is introduced about fundamentals of BLDC motor system. It includes BLDC mechanical structure and relevant motor drive circuit, sensored and sensorless feedback system, and mathematical model of BLDC motor.

3 MOTOR CONTROLLER DESIGN REQUIREMENTS ANALYSIS

3.1 Motor Control Section

As shown in the figure 8, the motor controller needs to achieve normal operation, and at least six states of power-on reset, self-test, operation, commutation, speed regulation and fault protection are required.
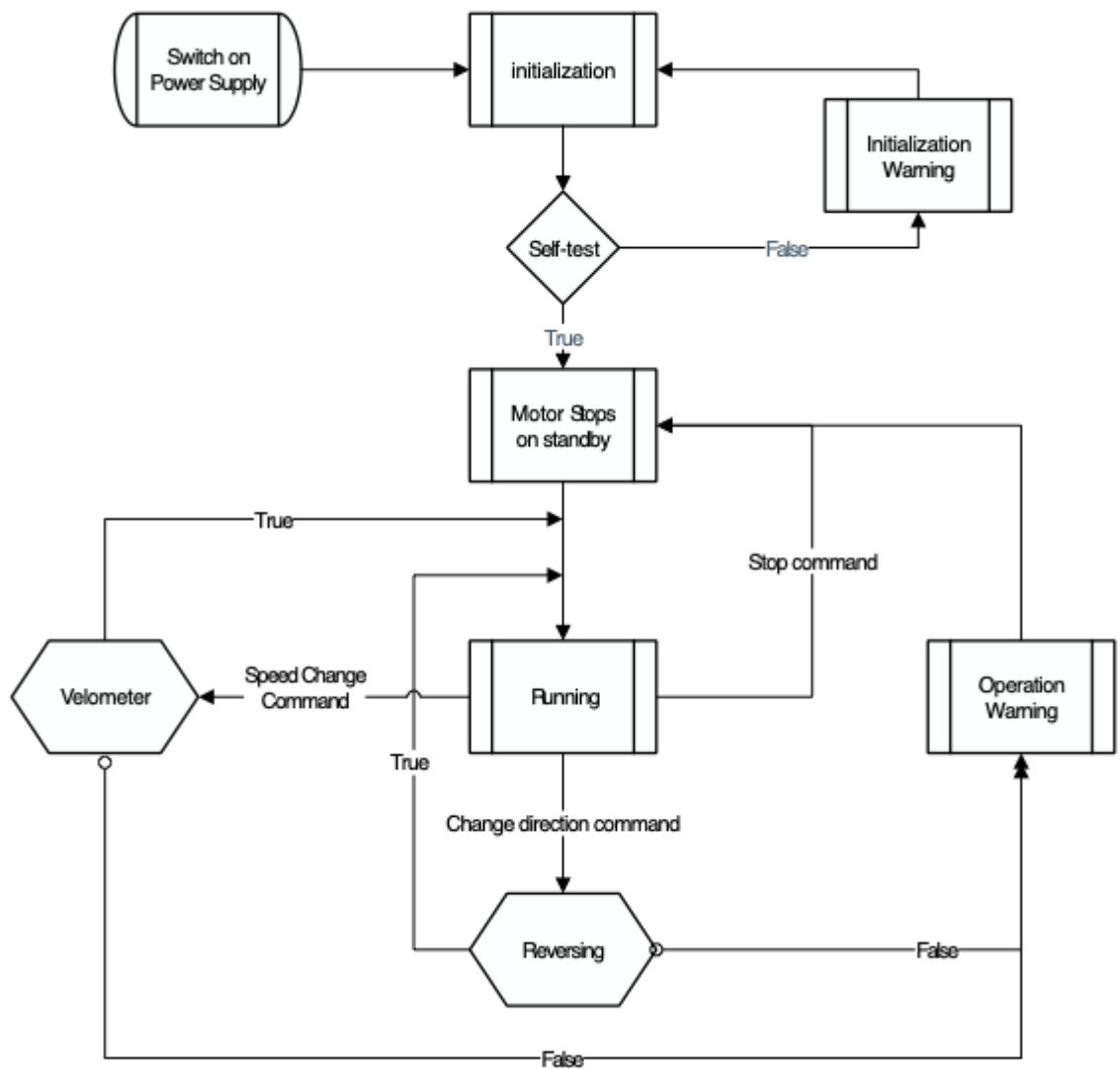
Figure 8. Main State Structure of Motor Control.

3.2   Open loop and closed loop control system

The control system of the brushless DC motor can be divided into an open loop control system and a closed loop control system.

The open loop control system is the simplest control system. It only includes the rotor position sensor which is used to provide feedback information on the rotor position, so that the motor commutation is always synchronized with the rotor position. The speed and current of the motor are determined by the mechanical characteristics of the motor and the driven load. If the voltage or load changes, the speed of the motor will change, and it cannot be controlled.

For the closed-loop control system, setting a common speed and utilizing a current double closed-loop control system can obtain better control performance. The block diagram of this design is shown in the figure 9. It can be achieved speed adjustment or steady speed control within a certain range.
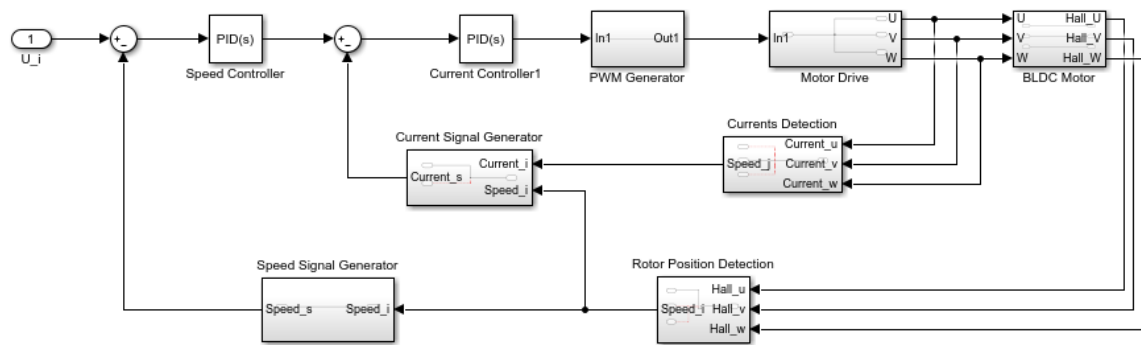
Figure 9. BLDC Motor Speed/Current Double Closed Loop Control System.

This system requires speed feedback and current feedback, so you need to set the speed sensor and current sensor. Its working principle is: first compare the input voltage (U_i) with the speed feedback signal (Speed_s) to obtain the speed difference and send this value to Speed Controller. A first stage adjusted output can be obtained then combine with the Current Signal, the second stage adjusted output can be obtained. After the PWM Generator analysis generates a control signal with a suitable duty cycle to the drive and then the drive produces the corresponding required output, so that the motor reaches the predetermined speed and current requirements.

In addition, the system also uses the feedback information of the rotor position to generate a composite signal (Current_s) representing the motor torque on the current sensor feedback signal for maintaining the phase of the opposite electromotive force and the phase current. The double closed-loop control system can make the motor automatically adjust under the condition of voltage, load change or external disturbance, so that its speed can track and reproduce the speed command requirements.

From a design perspective, it is necessary to verify the function of the open-loop control system before building a closed-loop control system. This is to improve the reliability of the system and prevent hardware or other interference factors from affecting the adjustment of

the closed-loop control feedback. Therefore, we must first implement the open loop control system testing.

3.3   Self-test and early warning function design

To ensure the normal and safe operation of the system, and to prevent failure or failure of secondary accidents caused by uncontrollable factors, self-test and early warning design is essential. Except the hardware protection circuit, the software's self-test and early warning functions can also effectively prevent failures.

The self-test function needs to include power, clock, I/O status, interrupt status, and initial motor position as required by the design environment. The warning function requires a warning mechanism for over-voltage protection, over-current protection, speed protection, command failure and sensor abnormality. As is shown in the figure 10.
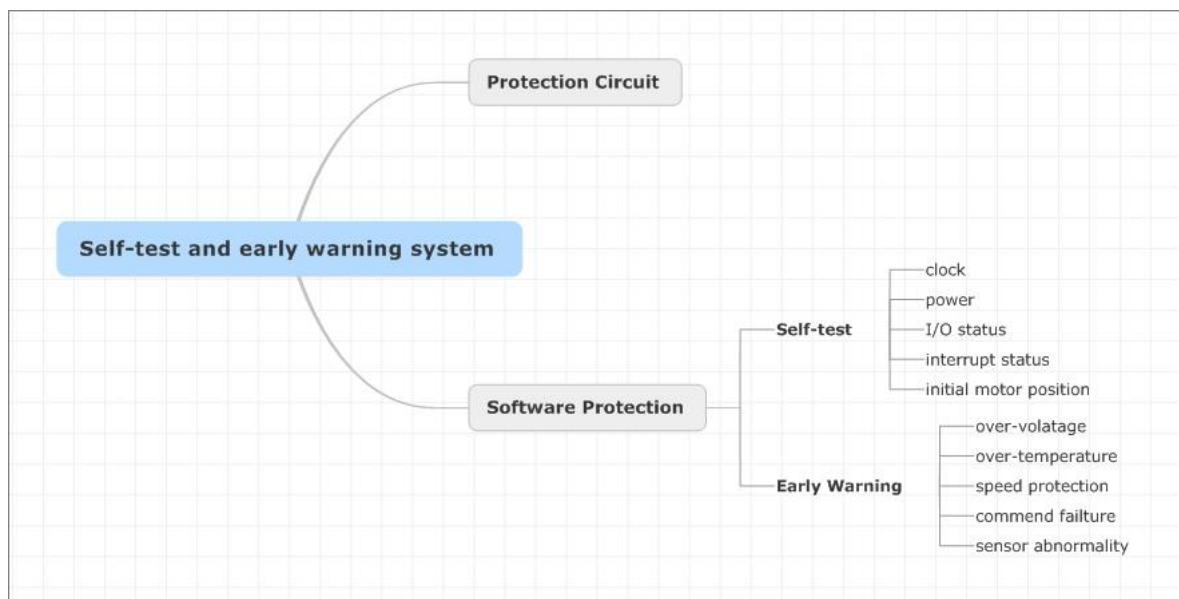
Figure 10. Self-test and early warning architecture design.

The driver is usually composed of power switch components(such as IGCT, MOSFETs, IEGT, etc.) to form a bridge inverter circuit or a non-bridge switch circuit. These components must be strictly followed in a certain order of use, otherwise it is easy to damage the components and fail. Therefore, it is important to self-test the status of each port of the controller to which it is connected before operating the drive.

During the operation of the motor, it may be damaged by electrical components due to excessive load or extreme working conditions such as high temperature, humidity or dust. The most common are component burnout and breakdown caused by high temperatures and high currents. In addition, the closed-loop control of the driver is based on the feedback signal of the sensor. If the sensor fails without warning, the motor will run in an uncontrolled dangerous state.

3.4   Summary

In this chapter, the requirements of BLDC motor control are analyzed. It covers system functions, control program logic, open-loop and close-loop frame, self-testing and warning logic.

4   HARDWARE DESIGN

4.1   Overview

To design a compact, high-efficiency, and reliable brushless motor driver, in addition to the basic functions, in addition to the basic functions, the smaller components should be selected under normal operating conditions.

For the design of the overall architecture, the choice of power supply must also be considered. A single power supply strategy can be considered without interfering with the normal operation of other components. Using a single power supply will reduce the extra power supply cable, and the drive can be installed in a smaller space. However, the power protection circuit design must be strictly performed, otherwise it will easily cause multi-level chips burnout. In addition, the controller needs to have input and output ports suitable for motor control and certain computing processing capabilities and needs to reserve a certain universal communication interface to adapt to a wider range of applications.

4.2   STM32F107VC Micro-controller

The STM32F107xx connectivity products, which is in STM32F10xx family that is widely used in industrial control, embedded equipment, in-vehicle system and motor control, is one of the high-performance ARM Cortex-M3 32-bit Micro Controllers of ST Company. It has a range of advanced communication interface, such as two I2Ss, three SPIs, two CANs, especially the Ethernet. The STM32F107xx products offer an IEEE-802.3-2002-comliant access controller (MAC) for ethernet LAN communications, which can be applied in modern embedded system communication technology flexible [21-22].

The primary features are [23]:
- 32-bit Cortex-M3 ARM MCU
- Maximum frequency reaches to 72MHz
- High performance single-cycle multiplication
- High performance Timer and Interrupt System
- Up to four 16-bit timers each with input capture, PWM and encoder input

- One 16-bit advanced motor control timer with dead -time control and emergency break
- Two basic timers
- Two watchdog timers
- One SysTick timer
- Various and flexible communication interfaces
- Two I2C interfaces
- Five USARTs
- Three SPIS
- Two CAN interfaces with 512 bytes SRAM
- Ethernet MAC with DMA and 4K bytes SRAM
-

As is shown in the figure 11.
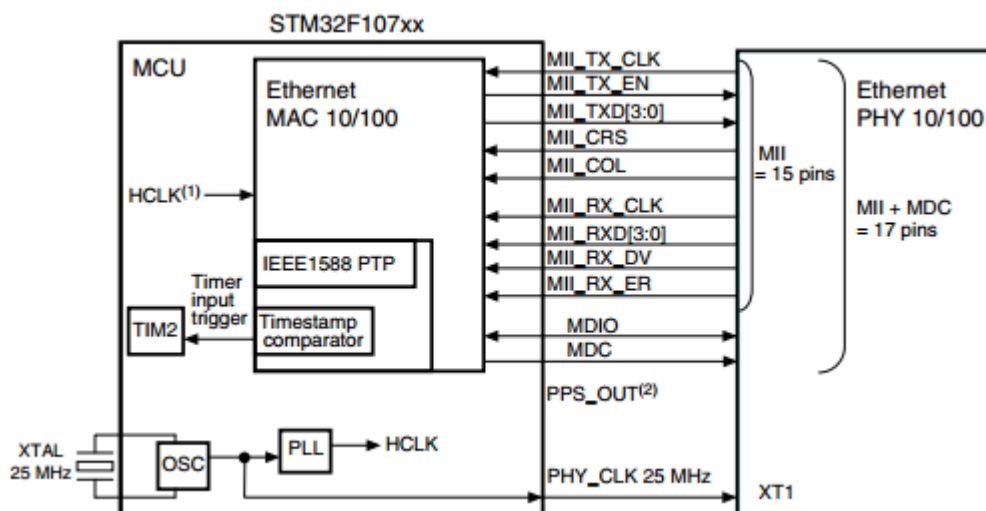
Figure 11. Ethernet interface solution.

The advanced motor control Timer (TIM1) is designed to provide a three-phase PWM multiplexed on 6 channels can combine with another timer TIMx (TIM2, TIM3 TIM4 or TIM5) with a Hall sensors interface to build up a close loop control part and drive BLDC motor. As is shown in the Figure 12.
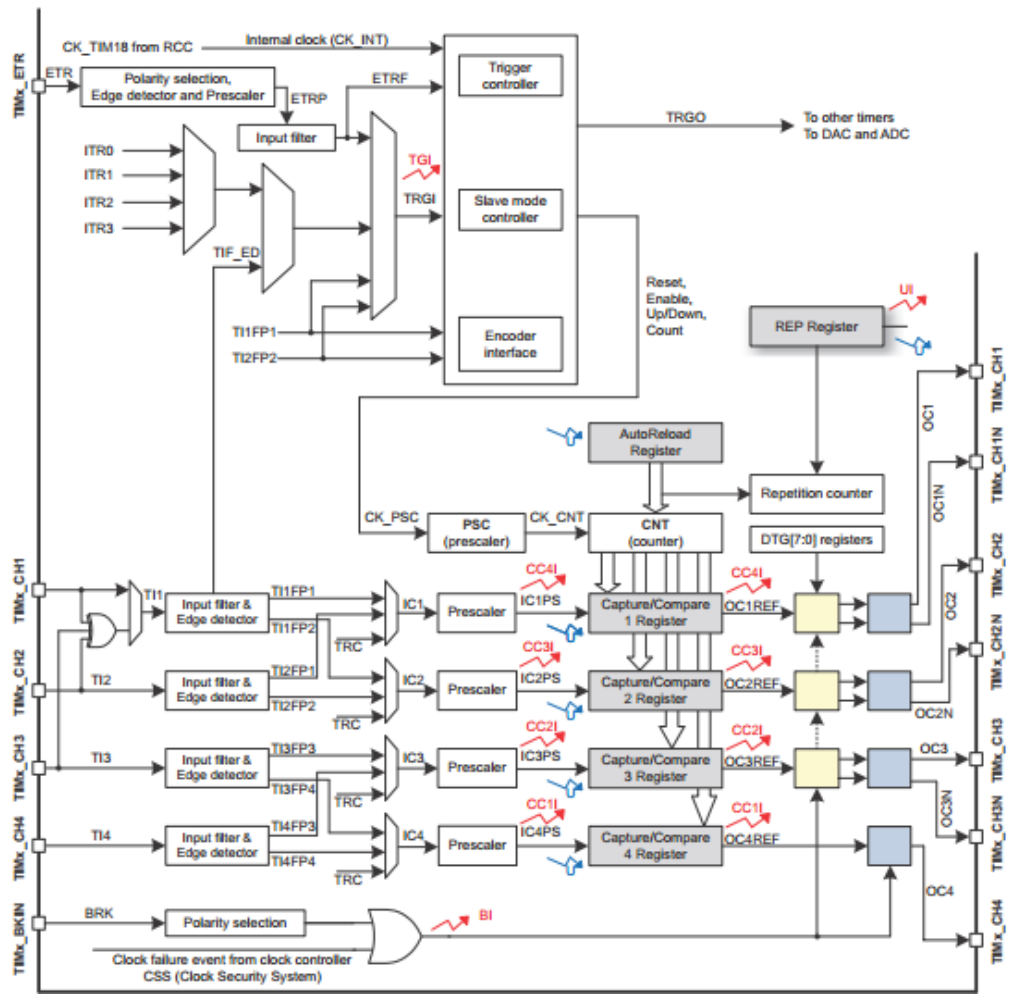
Figure 12. Advanced control timer block diagram.

4.3 Three-phase BLDC motor

The device used an 8-lines Brushless DC motor of STEPPERONLINE company with 24V operating voltage, 9A current and hall sensor. The specification of is shown in table 1 below.

Table 1. The specification of BLDC motor

Specification	Value
Number of phases	3
Number of poles	4
Related voltage (v)	24
Related current (A)	9±10%
Related power (W)	134
Related speed (rpm)	3500±10%

| Sensor	Hall Sensor
Insulation resistance	100MΩ@ 500VDC

4.4   DRV8332 Motor Driver

The DRV83323 is a high integrated three-phase DC motor drivers with an advanced protection system. The efficiency of this motor driver can reach up to 97% because of the low $R_{DS(ON)}$ of the power adjustor MOSFETs and gate drive design. The body size is 15.90mm × 11.00mm. This high integrated and efficiency makes it possible to use for a smaller power supplies and devices with a good energy-efficient application, is selected to apply in this project[24-25].

The main features are:

- High-efficiency power stage up to 97%
- Operating voltage up to 50V
- Up to 13A peak current and 8A continuous phase current
- PWM operating frequency up to 500kHz
- Independent supply and ground pins for each Half Bridge
- Integrated self-protection circuits including under-voltage, over-temperature, overload and short circuit

The DRV8332 has a unique independent supply for each half-bridge and these pins make it possible to provide current measurement through external shunt resistor and support half bride drivers with different power supply voltage requirements. Meanwhile, the DRV8332 provides three independent control PWM output ports, where adding a digital NOT gate between the high and low half bridges, as shown below, which means that we only need to output 3 PWM signals. This design ensures that the high and low half bridges in the same phase will never turn on during normal operation. This function reduces the problem of circuit damage caused by the error of the program test opening the in-phase high and low half bridge during the development process. By configuring the RESET_X pin to control the enable function of each phase, the phase control of each phase is independent of each other. As is shown in the figure 13.
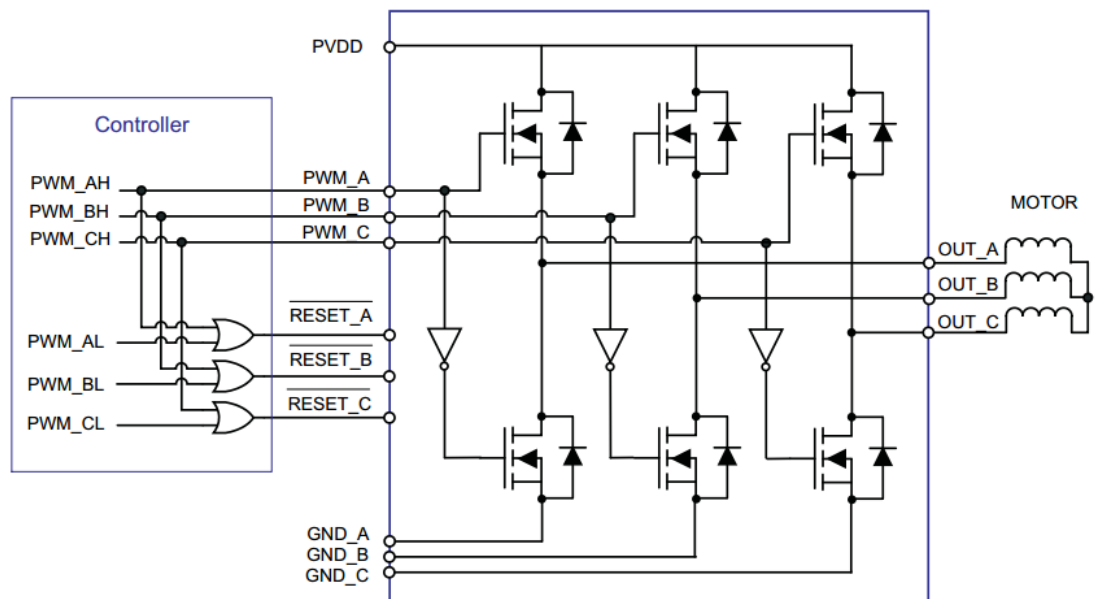
Figure 13. Control Signal Logic Input Scheme

4.5 Digital Design

The interface design of the controller should meet the control requirements of the driver chip DRV8332, and at the same time, the operating parameters of the motor must be considered. As table shown, the operating voltage should reach to 24V and the maximum current should below than 9A, corresponding to the specification of 8A continuous phase current and 13A peak current of DRV8332.

To drive the DRV8332, the controller needs to have 3 PWM_X outputs and 3 RESET_X configurations. In addition, the DRV8332 has overcurrent protection and overtemperature protection. The warning signals with two feedbacks need to be read by the controller. Therefore, the controller is connected to the drive DRV8332 with 8 interfaces.

Besides, Hall signal feedbacks of BLDC motor require three interfaces to be connected to the controller to ensure phase synchronization and speed detection and three ADC sampling interfaces are used to read the analog values of the current feedback. For building a compact high-power density driver design, the shape of the controller board should match the driver to reduce unnecessary space waste in the layout.

4.5.1 Power supply

There are three different voltages needed in the whole system.

24V power supply is applied to provide power to drive BLDC motor as power input PVDD; 12V power supply is asked for DRV8332 as power input GVDD. For STM32f107 micro-controller, the operating voltage is 3.3V but considering the requirements of peripheral devices, which are usually needed a 5V power supply, the 5V power supply is collocated and the most of SMT32 series micro-controllers have a 5V to 3.3V power regulator. Therefore, two stages power supply scheme is selected, and two power regulators are used here, as shown in figure 14.
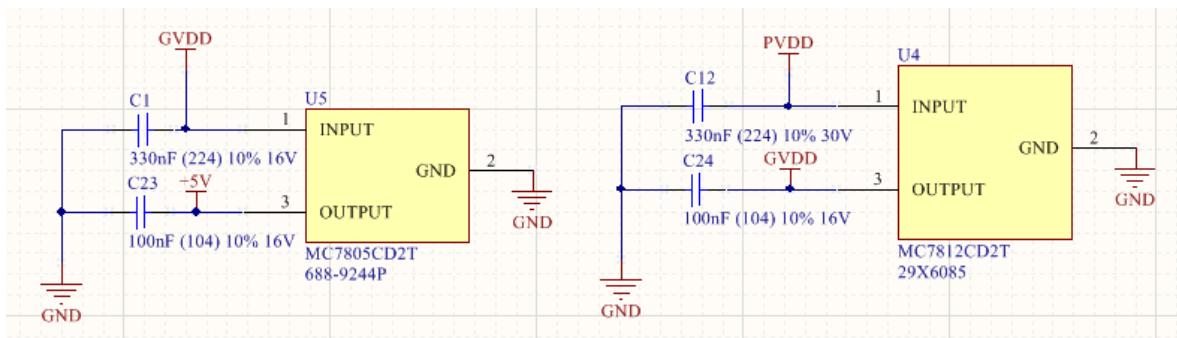
Figure 14. 24V to 12V (right) and 12V to 5V (left) Power Regulators.

The PVDD is the 24V power supply, which is as the single power supply used in the whole driver system and it is a DC power supply. MC7812 is a power regulator that can transfer power supply from 24V to 12V. The same as MC7812, MC7805 is the same series of power regulators produced by ON Semiconductor [26].

The first stage is that MC7812 uses 24V power supply PVDD as input and generates 12V power GVDD as output. Then the second stage uses this produced GVDD as input to regulate +5V power by MC7805. Both two regulators have 1.0A maximum output current that is enough to drive both DRV8332 operating, STM32f107 controller and Hall sensor power.

A 330nF or larger tantalum or mylar capacitor that has low internal impedance at high frequencies should be used to provide good high-frequency characteristics to insure stable operation under all load conditions. The bypass capacitor should be mounted with the

shortest possible leads directly across the regulators input terminals to minimize ground loops and lead resistance drops since the regulator has no external sense lead.

The MC7800 Series of fixed voltage regulators are built with overtemperature and overload protection in case of an excessive power overload condition. Besides, Internal Short Circuit Protection is designed to limit the maximum current the circuit will pass and Output Transistor Safe-Area Compensation that reduces the output short circuit current when the voltage across the pass transistor is increased. Considering these designs, external fuse does not apply in this design.

4.5.2 STM32F107 Module

The applied STM32F107VC micro-controller uses LQFP100 package, that has 100 pins with multiple functions, where is far beyond the conditions required for this design. In order to achieve a compact and high-power density design[21], select the compact layout design as shown in figure 15, while satisfying the function and preserving enough application interfaces while considering the shape of the drive.
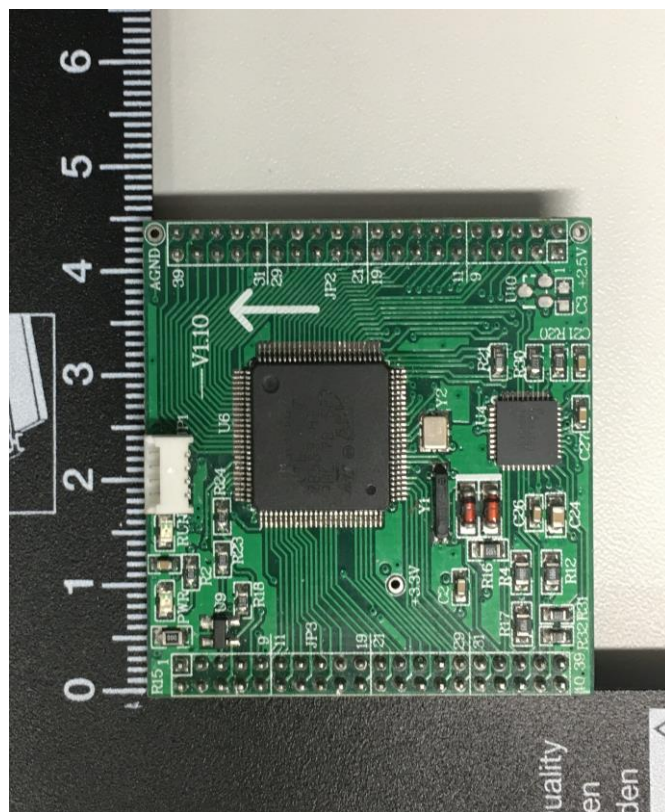

Figure 15. STM32F107 Module

The size of this module is 45mm × 45mm. It has 80 external pins. The multiplexed function pins are mapped to the normal I/O port by the remapping function. In this way, the number of ordinary I/O ports is reduced, and the utilisation of pins is also increased. The 4 timers, 9 ADC channels, SPI, UART, I2C, CAN, Ethernet and JTEG functions are saved. It integrates a 5V to 3.3V voltage regulator which can provide both these voltages output ports.

4.5.3 DRV8332 interface

According to its datasheet[26], the application of DRV8332 diagram is shown in the figure 16. PWM_A, PWM_B, PWM_C and RESET_A, RESET_B, RESET_C are input signal ports. FAULT pin can generate fault signal and OTW pin can set an overtemperature waring signal. An internal pullup resistor to VREG, which is 3.3V, is provided on outputs of them. The DRV8332 needs a 12V power supply GVDD to drive on and for output side a 24V DC voltage PVDD is to drive the BLDC motor.
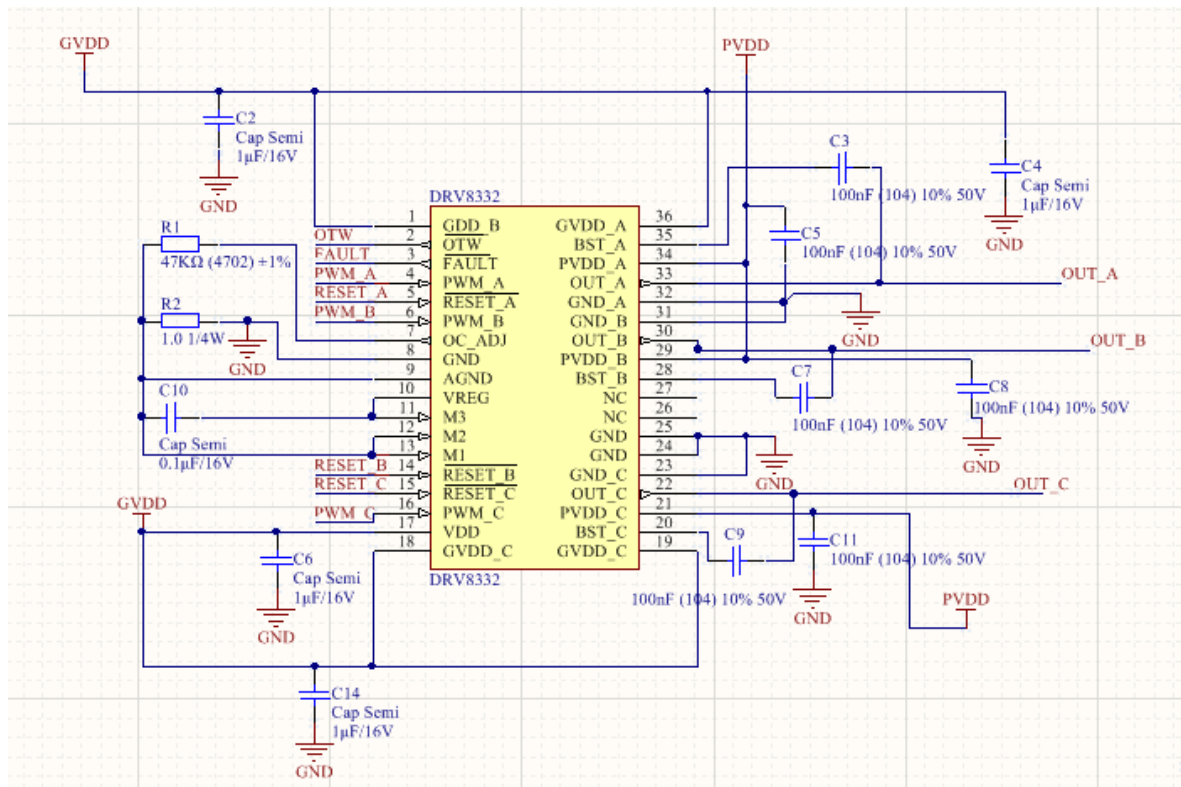

Figure 16. DRV8332 Interface

The overcurrent protection is designed by selecting an OC-Adjust resistor, the R1, to set the maximum current before overcurrent occurs. Considering the experiment condition, a 47kΩ

resistor is chosen and the corresponding maximum current is 5.8A. A 1Ω resistor is connected between GND and AGND to isolate the noise from board ground to AGND.

4.5.4 Feedback signals

The hall feedback signal and current detecting feedback signal are both used in this system as said before. Because the hall sensors are set inside of BLDC motor, there is no need to build external circuit but only provided +5V power and GND to support them to work. Therefore, the hall feedback signals interface can directly be set in figure 17.
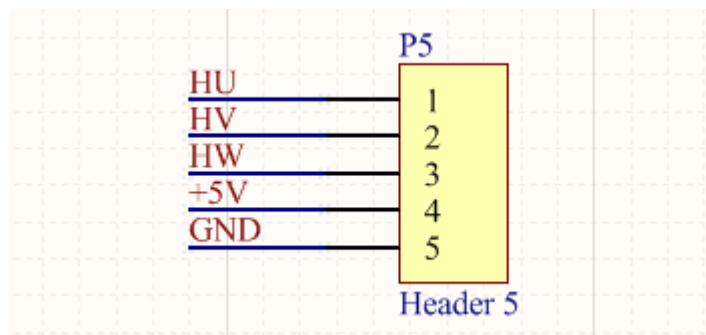
Figure 17. Hall feedback signals interface

The current feedback signal is calculated by calculating a voltage of 0.01Ω power resistors and dividing by the resistance value. The maximum sampling voltage of the ADC of the microcontroller is determined by Vref pin, which is usually equal to 3.3V. However, the output voltage is 24V. Here, an operational amplifier circuit is needed to obtain the sampling voltage allowed by the ADC. Since the ADC of the controller module has a voltage divider circuit, the maximum sampling voltage of the ADC can be set to 5V, as shown in figure 18.
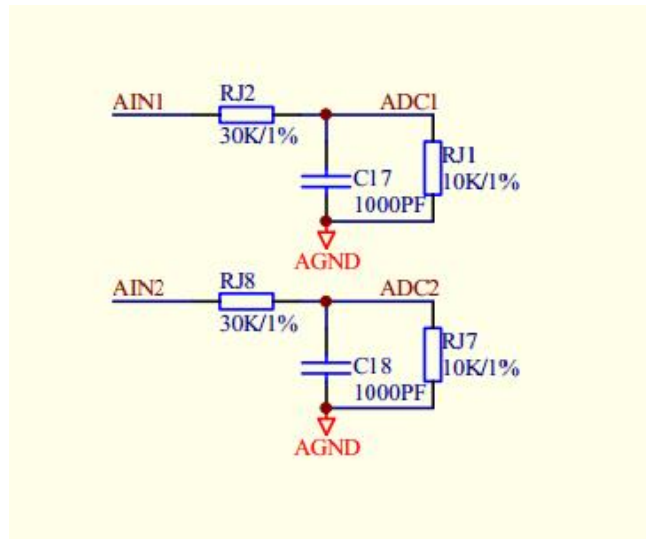
Figure 18. ADC sampling circuit of STM32f107 module

Considering that the motor's drive signal operates at a higher frequency, to ensure a more accurate and reliable sampling signal, a dedicated motor current sense amplifier LT1999-20 is used here. Take the C phase as an example, its schematic diagram is as follows in the figure 19.
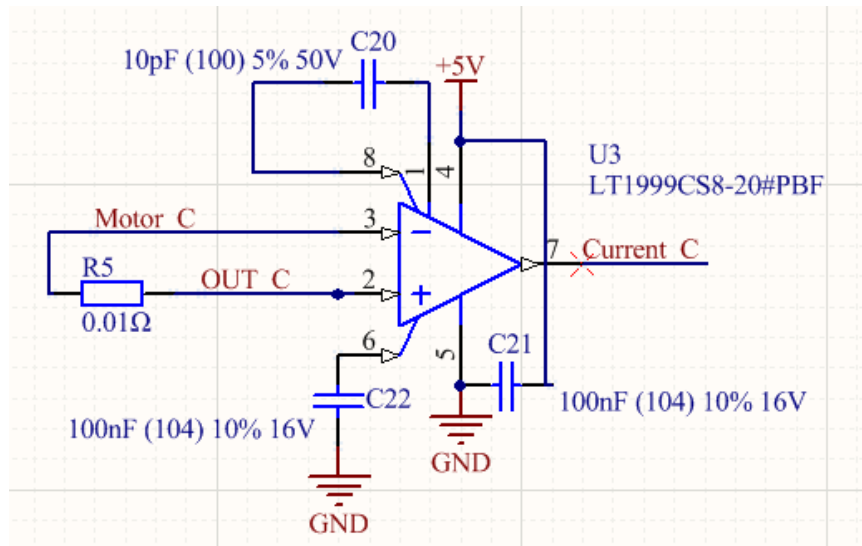
Figure 19. Current Amplifier Circuit of Output C

The LT1999 is a high-speed precision current sense amplifier, designed to monitor bidirectional currents over a wide common mode range[27]. The 0.01Ω power resistor is connected in parallel between the output OUT_X of the DRV8332 and the motor input MOTOR_X. The theoretical output voltage is determined by the sensed voltage (V_{SENSE}), and the ratio of two on-chip resistors:

$$V_{out} - V_{REF} = V_{SENSE} \times Gain \ (14)$$

Where

Gain is equal to 20 for LT1999-20.

Assume the operation current is 6A. The power loss on three power resistors:

$$P_C = I^2 \times R = 6^2 \times 0.01 = 0.36W \ (15)$$

$$P_t = \frac{2}{3}(P_A + P_B + P_c) = 0.72W \ (16)$$

Therefore, the power of the power resistors is chosen to be 1.0W.

4.5.5 Review

Overall, the total architecture is designed and shown in figure 20. This DRV8332 design includes DRV8332 driver, power regulators, current amplifiers and input/output signals interfaces.
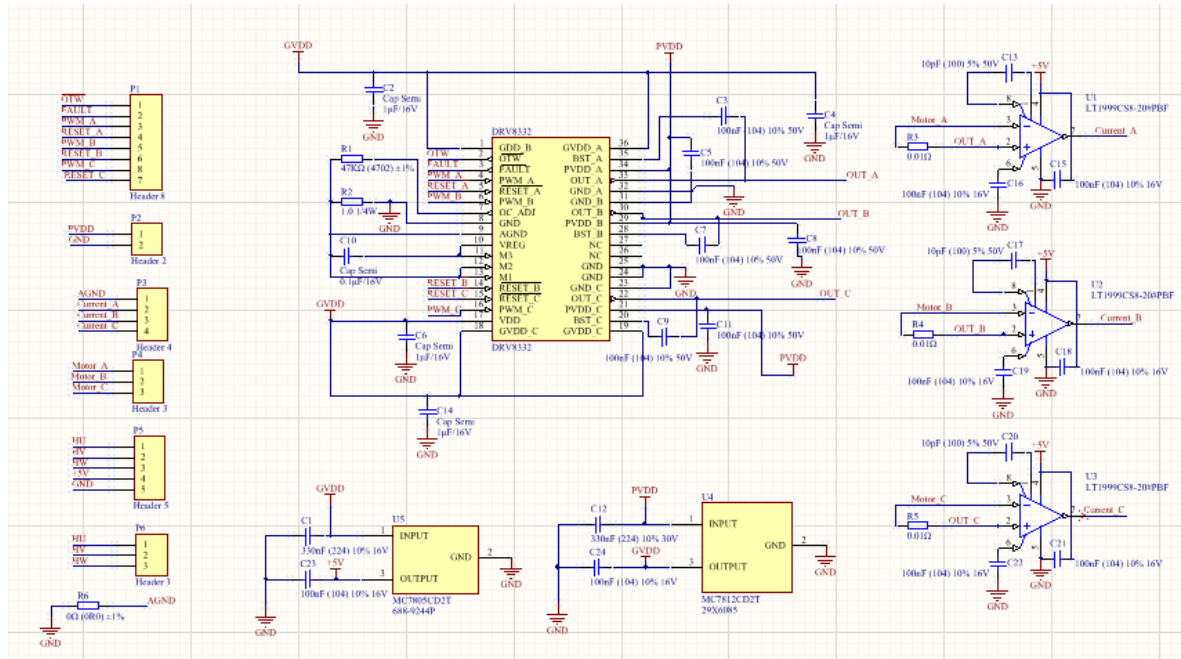
Figure 20. The Overall Structure of DRV8332 Module.

4.5.6 Experimental design

To verify the design more scientifically and effectively, it is necessary to gradually verify the above design and finally obtain feasible results. Independent function test completion is done on the breadboard.

The first stage for experiment needs to get the expected output signals of the controller independently, according to DRV8332 requirements. The controller needs to output three-way complementary PWM drive signals PWM_A/B/C and three independent bridge control signals RESET_A/B/C. The warning signal fed back by the driver is intended to be obtained and designed to protect the solution.

The second stage should connect with DRV8332 and the correct output from its should be verified. Then to drive the BLDC motor with Hall sensor, the detection of the Hall signal and the synchronization of the rotor of the motor should be implemented. In addition to this, it is necessary to verify the power supply scheme of the three-level power supply circuit. Additional controller peripheral development boards are also used to facilitate observation of experimental phenomena, as shown in figure 21.

Figure 21. Experimental circuit based on breadboard test

The static test described above is to ensure the logical correctness of the design. After verification on the breadboard, performance verification can be performed by designing the PCB board.

4.5.7 PCB board

Considering that the signal lines need to be away from the power lines to avoid interference with the transmission signal, and the voltage regulator modules are close to each other but leave enough space for heat dissipation, make a PCB design as shown in the figure 22.
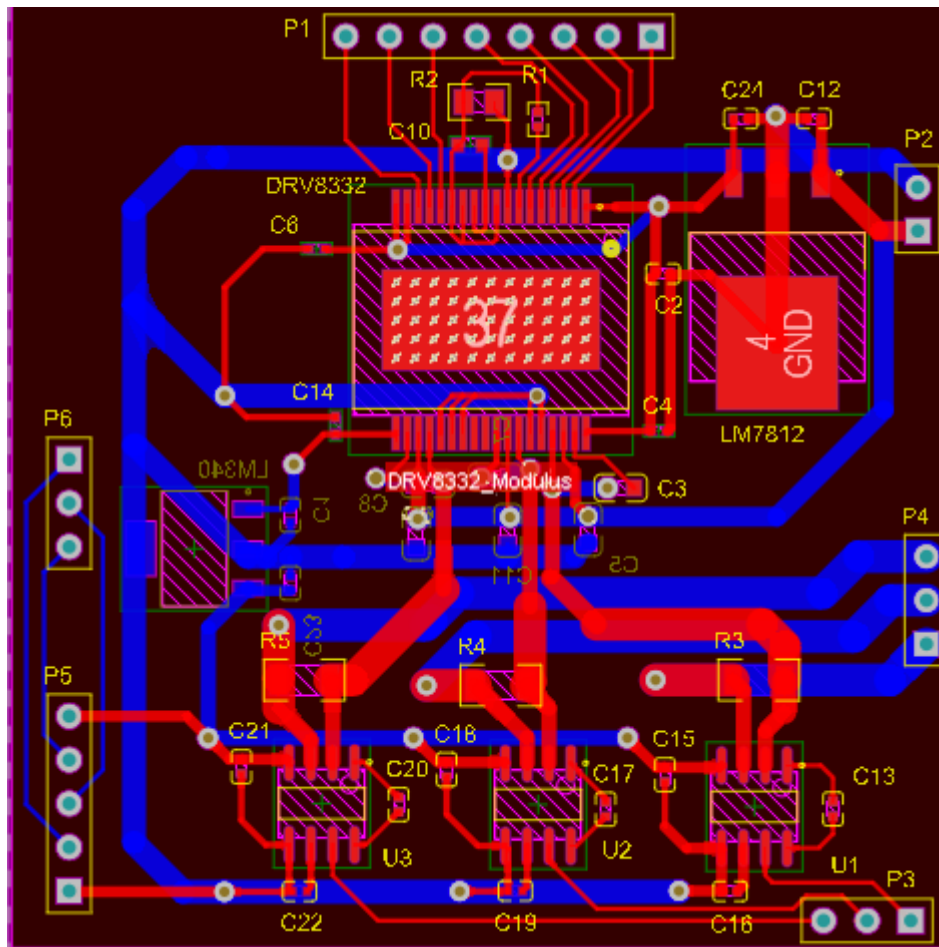
Figure 22. DRV8332 PCB Board Design

This PCB design with double layer board. The size of this board is 50mm × 50mm. The red lines are at the top of the layout and the blues are at the bottom side. The P1 interface is designed to transfer PWM control signals and the fault warning signals OTW and FAULT. All those signals relate to signal side of DRV8332. The P2 interface is used to be the input of 24V power supply PVDD and GND. It comes across LM7812 directly and generates a 12V power GVDD on top side to support and drive DRV8332 to work. In addition, 24V power transfers to output side of DRV8332 from bottom side. The three-phase output relate to both P4 interface and three power resistors R3, R4, R5 individually. The U1, U2, U3 are three current amplifiers. The current feedback signals are transited by the P3 interface. LM7805 is assembled on the left side of DRV8332 on bottom side. It provides 5V power to drive both amplifiers and Hall sensor. The P5 interface is used to support Hall sensor and transfer Hall feedback signals to P6.

To increase the area of the output line, copper is applied to the rest of the PCB to help reduce ground impedance that may generate a large amount of spike current in a digital circuit, while providing a complete return path for high frequency digital signals and reducing wiring for the DC network. In addition, for the serious heat problem of the DRV8332, this can also function to increase or decrease heat dissipation. to improve the heat dissipation efficiency, several via holes are added to the bottom of the DRV8332 to cool the chip[28]. The top and bottom sides of PCB design is shown in figure 23.
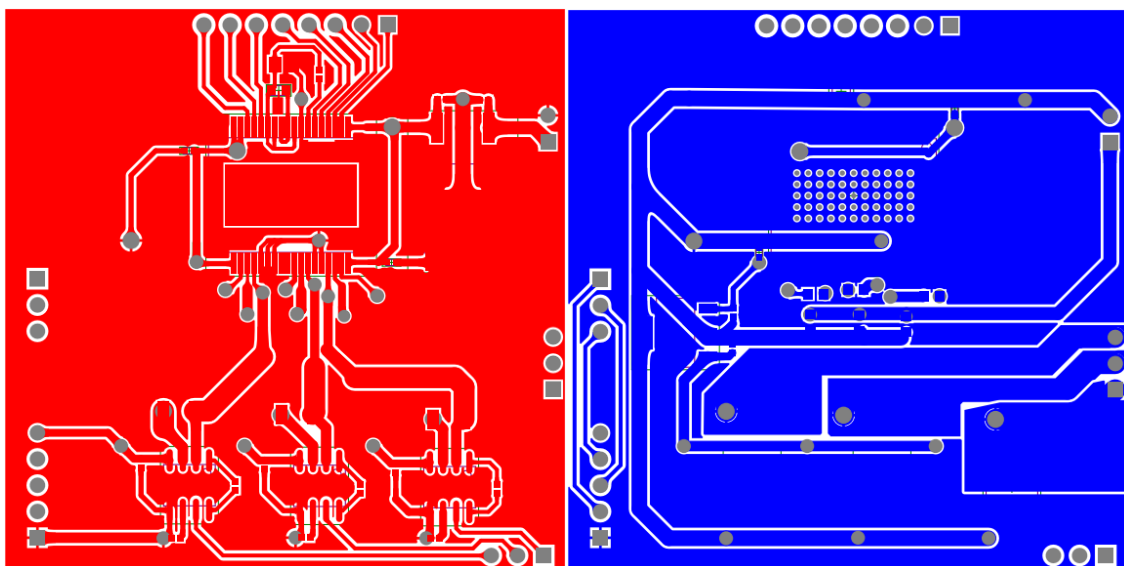
Figure 23. The Top (left) and Bottom (right) sides of PCB design

4.6   Summary

In this chapter, the whole hardware design is discussed. It includes microcontroller selection, three stage power supply scheme, motor drive chip selection, Hall sensor and current feedback signal interfaces of both framework and PCB circuit design.

5   SOFTWARE DESIGN

5.1   Overview

The design of the program is subject to the drive requirements of the DLDC motor and the DRV8332. The main drive 6 steps trapezoidal scheme logic with Hall sensor control is shown in figure 24.
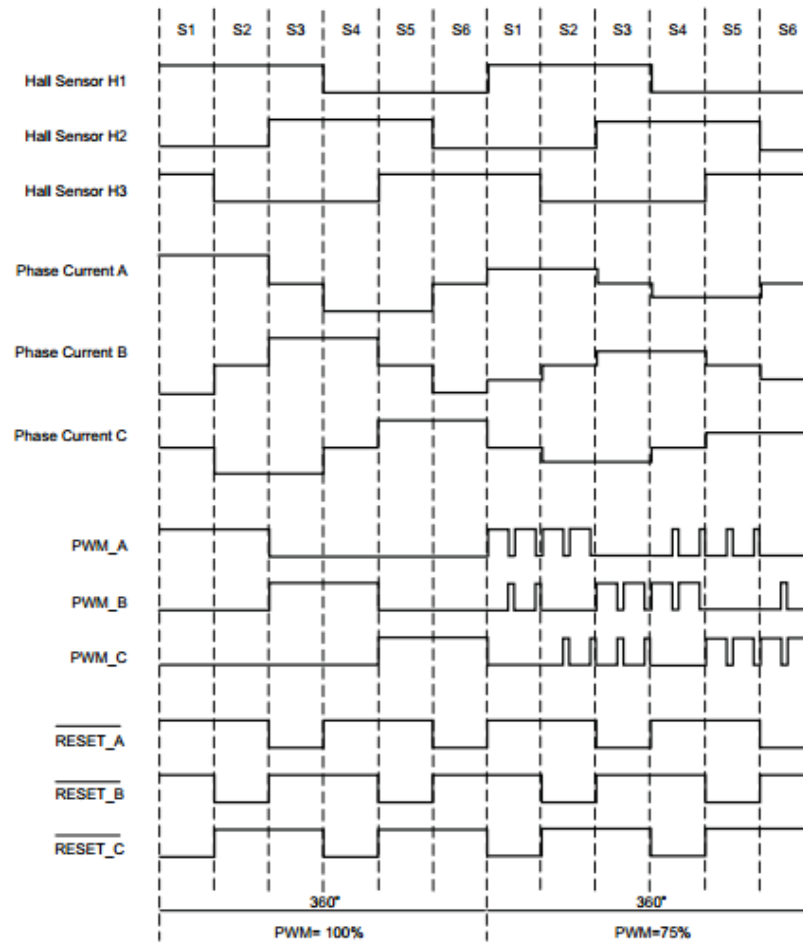
Figure 24. Hall Sensor Control With 6 Steps Trapezoidal Scheme Schematic.

Hall feedback signals are three-bit digital signals corresponding with six-step commutation. The table 2 describes the relationship between the sensor status and stator winding excitation.

Table 2. Commutation table of Hall sensor.

Hall sensors			Phase		
H1	H2	H3	A	B	C
0	1	1	-	NC	+
0	0	1	NC	-	+
1	0	1	+	-	NC
1	0	0	+	NC	-

1	1	0	NC	+	-
0	1	0	-	+	NC

5.2   Development environment

The developing is mainly based on two software: Keil MDK 5 and STM32CubeMX, which are the most powerful mainstream development tools of STM32 Series micro-controller. The programming language uses C language and for corresponding agile development the HAL driver layer, which provides a generic multi-instance simple set of APIs to interact with the upper layer, and it is covered by STM32Cube.

5.2.1 Keil MDK 5

Keil µVision MDK 5 is a window-based software development platform that combines a robust and mode editor with a project manager and make facility tool. It integrates all the tools needed to develop embedded application including a C/C++ compiler, macro assembler, linker/locator and a HEX file generator[29-30]. The following figure 25. shows the interface of Keil MDK User.
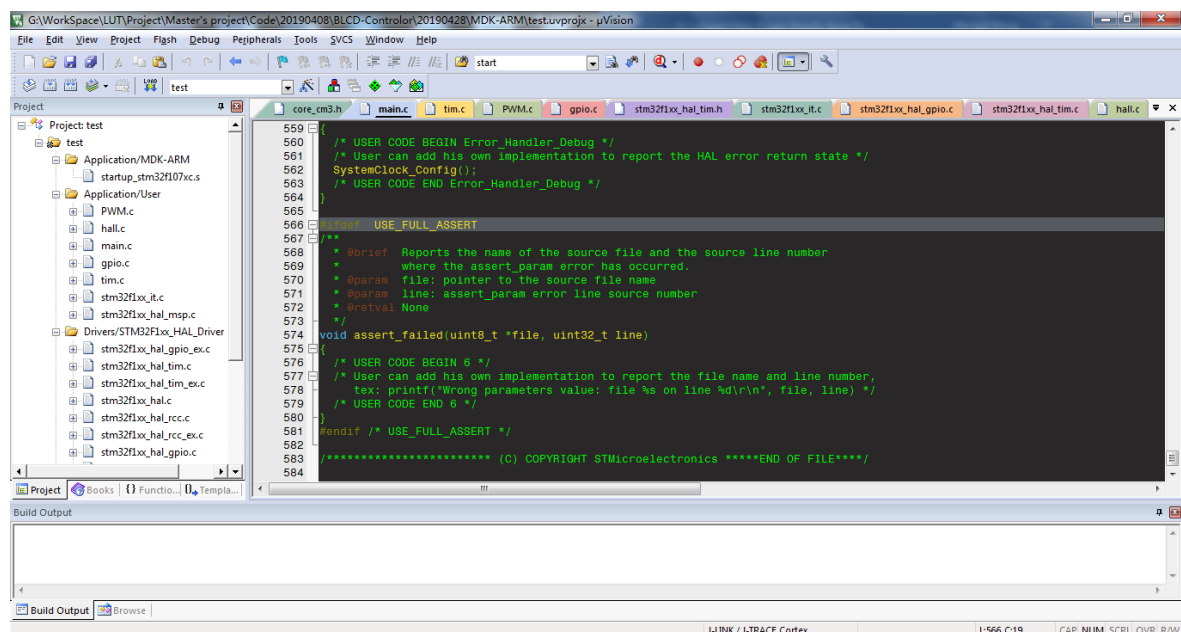
Figure 25. Keil MDK User Interface.

It has a powerful debug tool that can help in debugging and testing an application by using a debugger, such as J-link and ST-link, or simulator. The Keil MDK debugger can simulate

the behavior of the target application, for example, digital input, analog input and UART communication, that enables developers to test application prior to having the hardware.

5.2.2 STM32CubeMX

STM32 family products have a huge application functions that could be used in the different situations. However, the configuration is heavy work before building and applying a program. In addition, the time taken to migrate to new platforms and upgrade the code to the new firmware divers needs unnecessary delays to the project [31, 32]. According to the requirements of customers that need to quickly identify the controller and speed up development of program, ST company designed the new tool STM32CubeMX as shown in the figure 26.
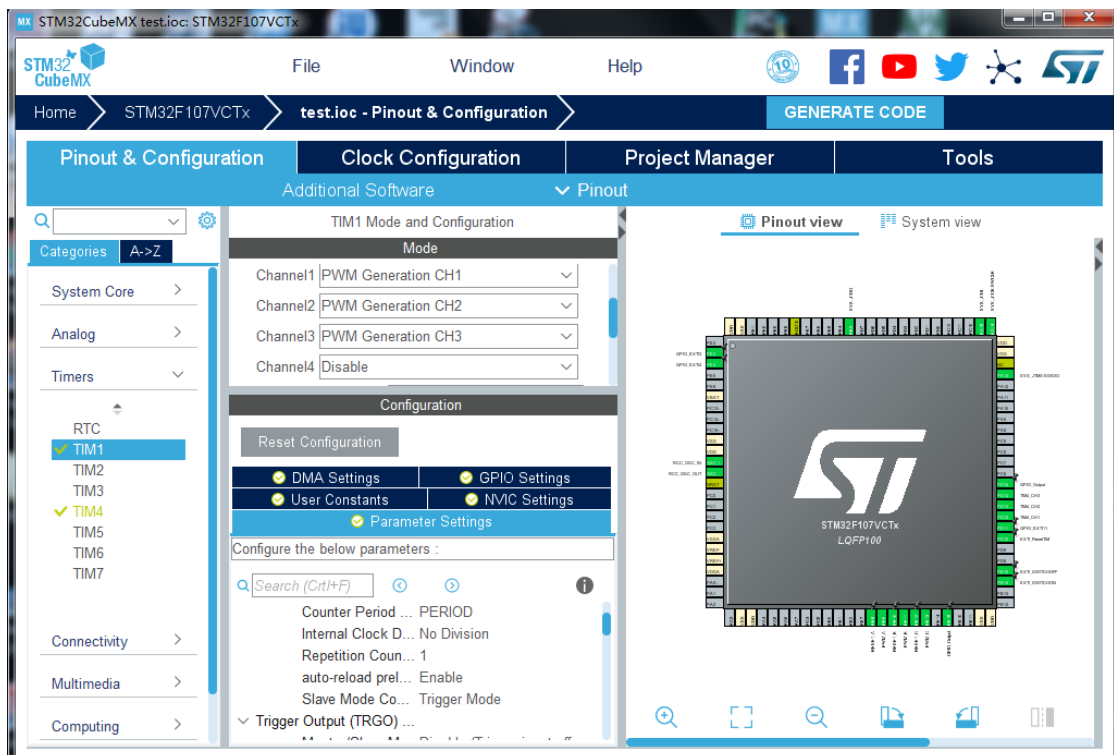
Figure 26. STM32CubeMX.

STM32CubeMX is a graphical tool for STM32 micro-controllers, which provides a highly efficient scheme to config registers and functions. The features of STM32CubeMX are:

- Fast and easy configuration of the MCU pins, clock tree and operation modes

- Complete project generation of the report of whole configurations for designers

- Power consumption calculation

- Easy transfer to other ST family platforms

- Easy advice for MCU selection

- Support of embedded software packages in CMSIS-pack format

- Interface of different IDE platforms (like MDK 5)

To adapt to the trend of micro-control programming and manage projects more effectively, the STM32CubeMX was used in this project.

5.3   Program architecture

The coding includes four main parts: the main function, interrupt configuration of signals generation, warning interrupt and communication control. The program flow chat is shown in figure 27.

(a)   (b)   (c)
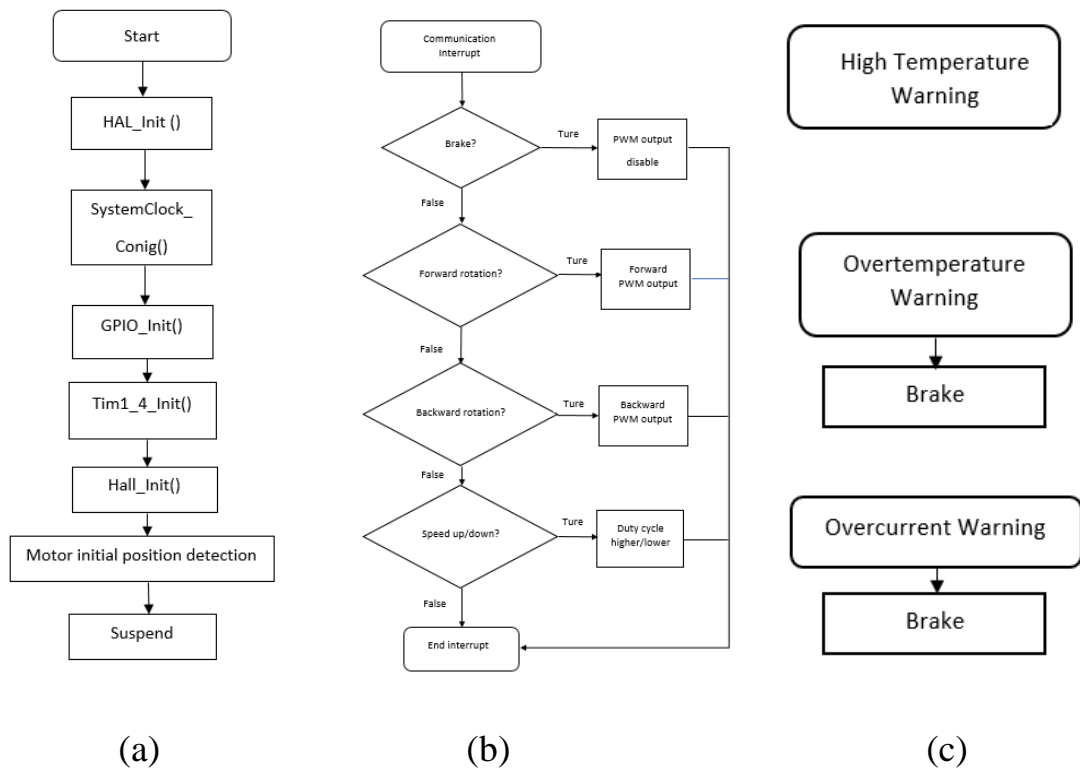
Figure 27. the Flow Chats of Main function (a);Communication Control with Signals Generation (b); and Warning Interrupt (c).

The main function is designed to initial program, including HAL driver remapping initialization, system clock configuration, GPIO interfaces initialization, timer 1 and 4 configuration, Hall sensor interface configuration and motor initial position detection. Each step has own self-test that does not mention here. Timer 1 is used to provide PWM wave signals to DRV8332 and timer 4 is the Hall sensor interface. After all initializations the program is suspended and waiting for the control commend.

Control signals are delivered by communication interrupt. It could be external triggers, UART communication event, CAN communication event or Ethernet data. Brake, forward rotation, backward rotation and speed up/down are the primary functions of control commends. Each signal has an operation response of specific requirement. Usually, it sets the related values of resistors to meet the demand during working period. The timer usually includes two registers: preload register and shadow register. Shadow register is the real operating register used when the program is running. Meanwhile, preload register could provide a configurating operation during that period and set a flag to shadow register. When timer comes to the next clock period, shadow register will update its values from preload register. By this way, those control instructions can be set without disturb output generating of PWM wave signals.

The external warning signals from OTW and FAULT output of DRV8332. Theses warning signals are set as external interrupts. The overtemperature protection system has two levels that assert an active-low warning signal OTW when the DRV8332 junction temperature exceeds 125°C and if the device junction temperature exceeds 150, the FAULT being asserted low and the device is put into thermal shutdown. The overcurrent warning signal will happen when the current through DRV8332 is higher than the mounted maximum current, described in the previous section, and, the device is being set into overcurrent shutdown.

5.4   PWM wave interface and generator

According to the figure 24., three channels of PWM generation and three enable output RESET_A/B/C are needed. Config the advanced timer TIM1 by STM32CubeMX as shown in figure 28.
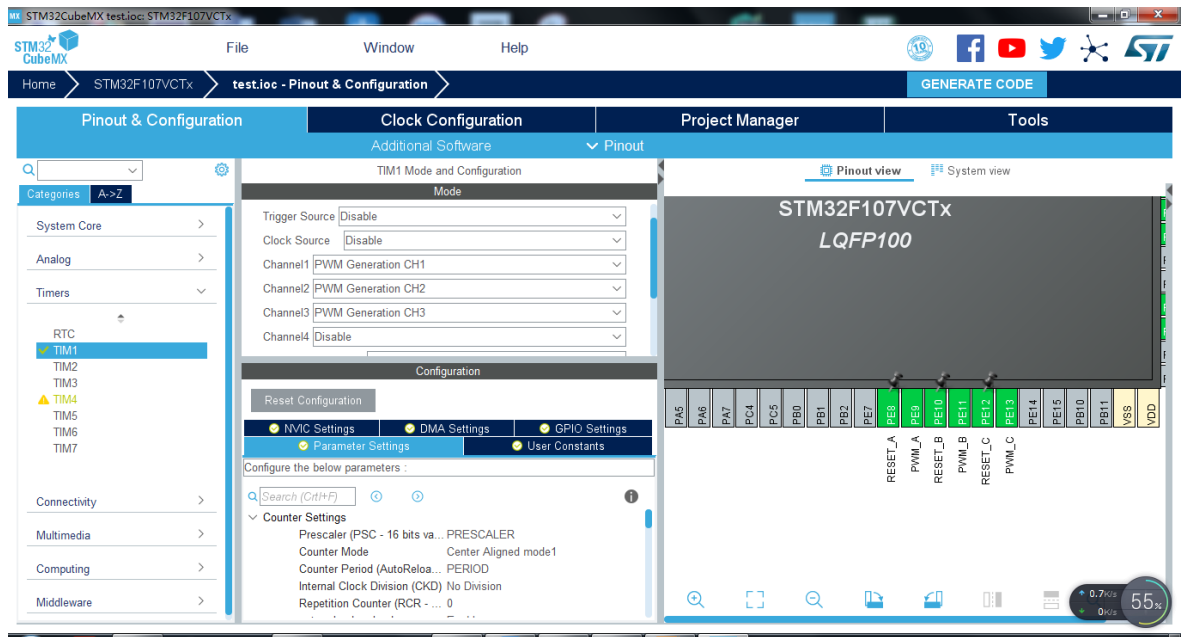
Figure 28. PWM generator configuration of TIM1.

Select PE8, PE10, PE12 as output ports and rename them as PWM_A, PWM_B and PWM_C . Remapping TIM1 output channels to these ports and set PWM generation function to each channel. Then set the parameters for TIM1. *Prescaler* is to modify the frequency and time base unit which will be used to calculate PWM period. The *Counter Period* is the pulse numbers generated in one timer period. And the *Pulse* of each channel is to determine the duty cycle of PWM. The system clock is selected to 72MHz of advanced peripheral bus (APB) line including TIM1. The duty cycle and one PWM pulse period are calculated as:

$$DutyCycle = \frac{Pulse}{ConterPeriod} \times 100\% \ (17)$$

$$Period = \frac{72MHz}{Prescaler + 1} \times CounterPeriod \ (18)$$

To produce bipolar PWM wave, which refers to the voltage passing through the two phases as being modulated with PWM. It means both the input and output of current are being modulated. To meet this acquirement, the polarity of each operating channel should be set complementary. The polarity represents the effective level after timer clock counter running beyond the configured Pulse in a Period. If the polarity is set as low, when timer clock counter is below than the Pulse, the output of this channel will be high and once counter is

beyond than this value, the output changes to the low. If the polarity is set to high, the opposite result will be obtained. In this way, the two-phase complementary output for each step could be achieved.

5.5 Hall Sensor driver

STM32Cube MX provides a default Hall sensor interface that is used in this program. Select TIM4 to be the sampling interface because it can tolerant maximum 5V input in case the device used in complex working condition. The configuration is shown in figure 29.
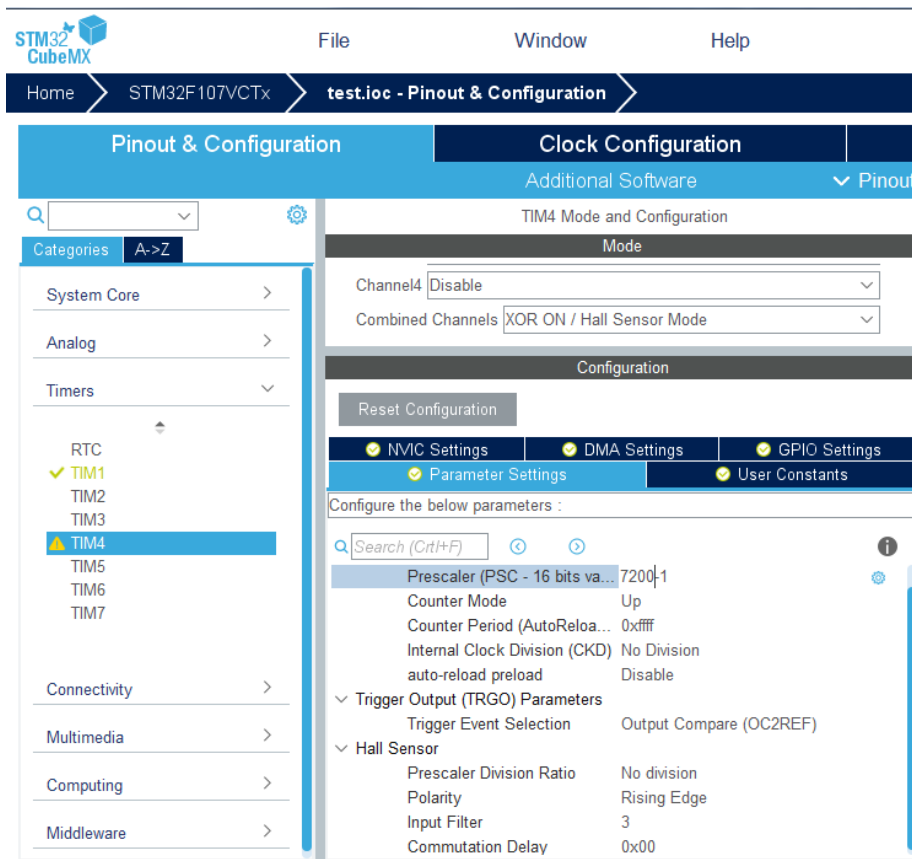
Figure 29. Hall Sensor Interface Configuration.

The three-way Hall signal is connected to the three channels of TIM4 and is triggered by an XOR gate to capture the compare interrupt. Hall signal detection mode is triggered by rising edge with a input filter. Set the maximum value 0xffff to counter period because the counter must be cleared by Hall signal XOR operation.

Each time the motor rotor makes one revolution, it will produce 12 Hall signal changes. Assume that the motor works at a maximum speed of 3500 rpm, Hall signal generation frequency f_{Hall} can be written as:

$$f_{Hall} = \frac{3500rpm}{60} \times 12 = 700Hz \ (19)$$

Hall signal sampling rate $f_{Sampling}$ can be shown as:

$$f_{sampling} = \frac{72}{Prescaler + 1} MHz = 10kHz \gg f_{Hall} \ (20)$$

Where

$Prescaler$ - the prescaler coefficient based on 72MHz bus clock.

Such sampling frequency satisfies the sampling needs of the Hall signal.

5.6   Speed calculation

The strategy for speed calculation is to calculate the number of pulses n generated during the period in which the Hall signal changes. The time each pulse is generated is a fixed constant. Its period is one period of the timer clock. It can also use TIM4 to calculate the motor speed. The period of one pulse T_{pulse} can be derived by:

$$T_{pulse} = \frac{1}{f_{sampling}} = \frac{1}{10kHz} = 100\mu s \ (21)$$

Define an overflow counter C_{over} to calculate the time when there is no Hall signal interrupt in a timer counter period. The initial value of C_{over} is equal to 1 and once the timer generates an overflow interrupt, this variable is incremented by one. Then, the rotate speed V is equal to:

$$V = \frac{(n + C_{over} \times 65535) \times T_{pulse}}{12} \times 60 = 5T_{pulse}(n + C_{over} \times 65535)rpm \ (22)$$

5.7   Current feedback interface

ADC1 is selected to be the current feedback interface. Config the function as shown in figure 30. by STM32CubeMX.
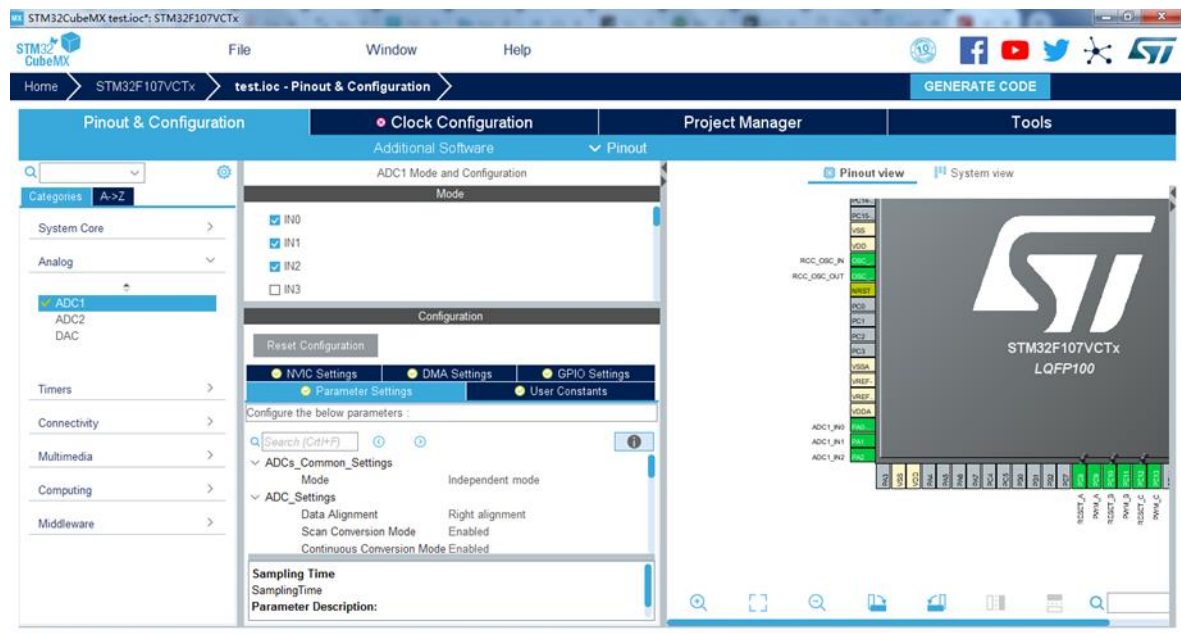
Figure 30. ADC Configuration of current feedback.

IN0, IN1, IN2 are selected as input port remapping as PA0, PA1, PA2. Set ADCs mode as independent mode. The data alignment is right alignment. The scan conversion mode and continuous conversion mode are enabled. Set number of conversions as 3 and each conversion uses a channel. Enable DMA Channel 1 and config direction as peripheral to memory, that can finish the communication of ADC without blocking other program by using DMA function.

5.8   The code of main function

The main function of the program is used to initialize the device and configure the corresponding interface.

```
/*
 * @file: main.c
 * @brief: Main program body
```

```c
    */
   int main(void)
   {
    /* MCU Configuration---------------------------------------------------*/

    /* Reset of all peripherals, Initializes the Flash interface and the Systick. */
    HAL_Init();
    /* Configure the system clock */
    SystemClock_Config();
    /* Initialize all configured peripherals */
    MX_GPIO_Init();
    MX_TIM1_Init();
    MX_TIM4_Init();
    /* Initialize interrupts */
    MX_NVIC_Init();
    /* Initialize Hall interface  */
   HallInit();
   /* Suspend  */
   Motor_Suspend();
    while (1)
    {
    }
   }
```

The control of the three complementary outputs is triggered by the Hall signals and reads the corresponding rotor position and then config it in the input capture interrupt.

```c
   /*
    * @function: Input capture interrupt of TIM4
    * @brief: Configure the mode of the output channel by reading the Hall signal
    */
   void HAL_TIM_IC_CaptureCallback(TIM_HandleTypeDef *htim)
   {
           uint16_t HallPhaseA = 0,HallPhaseB = 0,HallPhaseC =0, Hallstate =0;
```

```c
        /* Read Hall sensor state  */
        HallPhaseA = HAL_GPIO_ReadPin(GPIOD, GPIO_PIN_12);
        HallPhaseB = HAL_GPIO_ReadPin(GPIOD, GPIO_PIN_13);
        HallPhaseC = HAL_GPIO_ReadPin(GPIOD, GPIO_PIN_14);
        Hallstate = (HallPhaseA<<2) + (HallPhaseB<<1) + (HallPhaseC);
        /* Calculate rotate speed  */
        Speed=5*0.0004*(__HAL_TIM_GET_COUNTER(&htim4)+Counter_over*
65535);
        if(htim == (&htim4))
        {
           switch(Hallstate){
                        case Hall_S1:{ Output_S1(); break;}
                        case Hall_S2:{ Output_S2(); break;}
                        case Hall_S3:{ Output_S3(); break;}
                        case Hall_S4:{ Output_S4(); break;}
                        case Hall_S5:{ Output_S5(); break;}
                        case Hall_S6:{ Output_S6(); break;}
           }
}
/*
 * @function: External interrupt
 * @brief:  Carry out control instruction and handle warning signals
 */
void HAL_GPIO_EXTI_Callback(uint16_t GPIO_Pin)
{
// Forward rotate
        if(GPIO_Pin == GPIO_PIN_14)
                    Forward_rotate(Hall_State_Detect());
//Backward rotate
        if(GPIO_Pin == GPIO_PIN_15)
                    Backward_rotate(Hall_State_Detect());
//Suspend
        if(GPIO_Pin == GPIO_PIN_10)
```

```
                    Motor_Suspend();
    //Overtemperature warning
            if(GPIO_Pin == GPIO_PIN_0)
                        OTW();
    //FAULT warning
            if(GPIO_Pin == GPIO_PIN_1)
                        {FAULT(); Suspend();}
    }
```
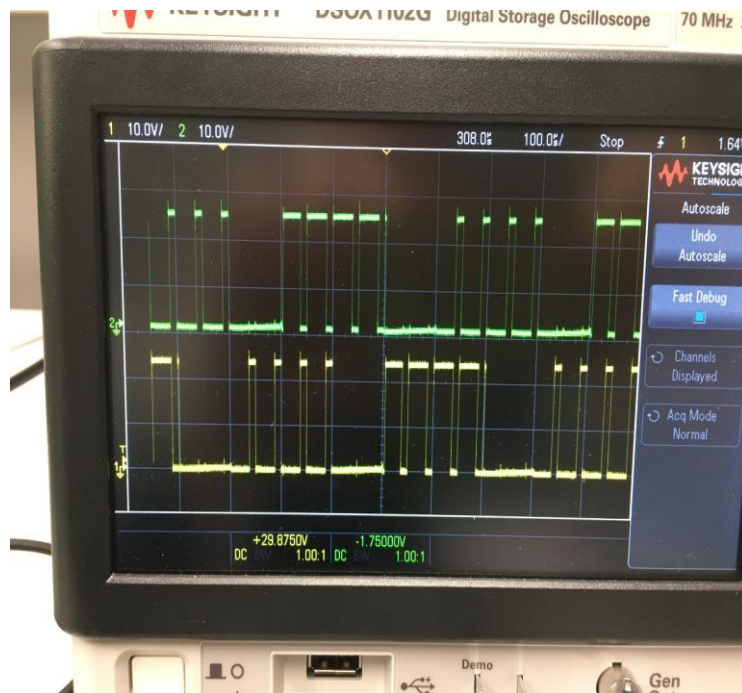
6   RESULTS

6.1   The result of PWM_A and PWM_B waves simulation of STM32F107

The first phase of the test is based on the controller's output signal. As shown in figure 31.,
the input signals of oscilloscope are PWM waves of phase A and phase B with a 75% duty
cycle. This simulation is performed by setting a fixed-cycle timer interrupt.


Figure 31. The result of PWM_A and PWM_B waves simulation of STM32F107.

This simulation result basically conforms to the requirements of the DRV8332 chip drive
timing diagram and verifies the feasibility of the controller driver.

6.2   The result of DRV8332 output

Load the previously mentioned PWM signal to the input of the DRV8332 while adding the stage driven by the Hall signal. Connect the three OUT (OUT_A/B/C) ports of the DRV8332 to the oscilloscope and output the single stage at 60% duty cycle as shown in figure 32.
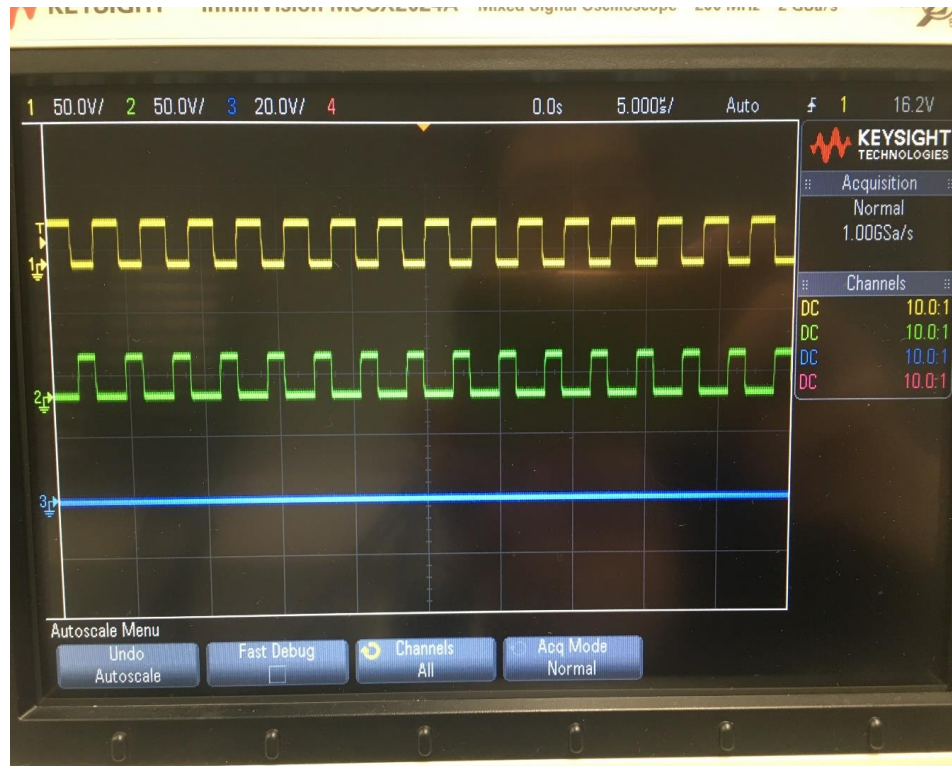

Figure 32. The three phase outputs of DRV8332 with 60% PWM duty cycle and deadtime insertion.

In the static program test, the complementary PWM wave signal is smoothed and there is no noise. To prevent the wear and breakdown of the internal MOSFETs of the chip, deadtime control is added to the output signal. The detail is shown in APPENDIX 4. Therefore, such outputs can be considered as the stable and reliable signals and can be output to the motor.

## 6.3   The three-phase outputs to BLDC motor driven by Hall sensor signals

Applying PWM output signals of DRV8332 driven by hall sensor signals. The corresponding warning system is used. The three-phase output voltage are shown in figure 33. The driving signals of the voltage are composed of the mentioned PWM waves before.
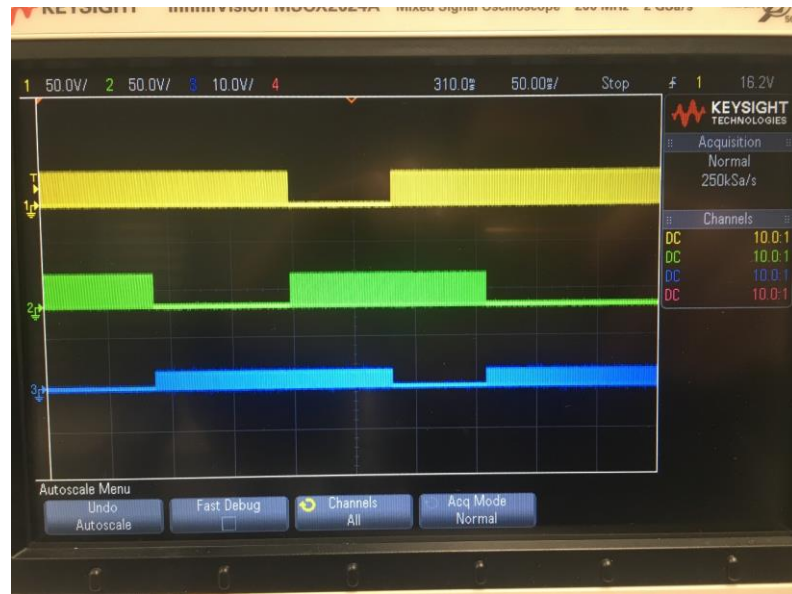
Figure 33. The six steps complementary input voltages of motor.

6.4   Speed control

The speed is calculated by Hall signal interrupt and timer period. The value is collected by UART and the speed curve is shown in figure 34.
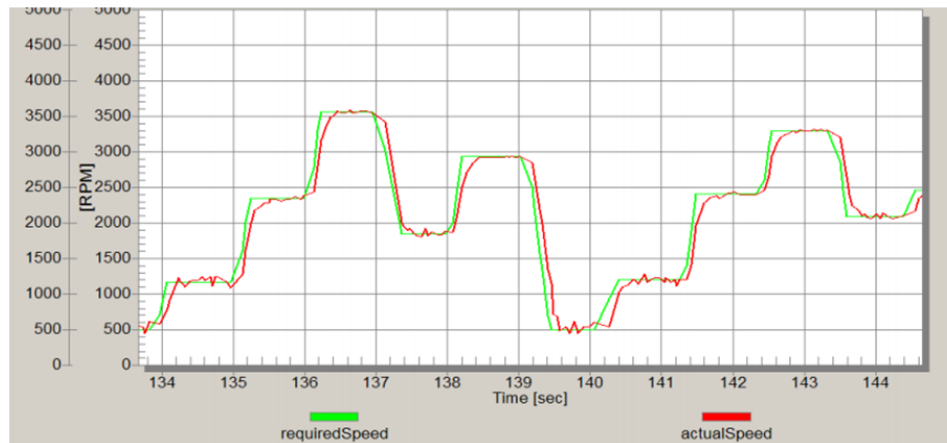
Figure 34. Speed response curve of BLDC motor.

Change the motor speed by setting a predetermined speed command. Adjust the voltage by changing the duty cycle of the PWM wave to further adjust the motor speed. The actual speed of the motor has basically reached the predetermined requirements. However, it will fluctuate when approaching the predetermined speed.

7 CONCLUSION

7.1 Summary of research

This thesis focuses on the implementation of a compact BLDC motor drive.

In the chapter 1, we discuss the whole brushless DC motor system, which includes microcontroller, motor driver and BLDC motor. And the development is discussed at the next, involved motor body, control algorithm and drive circuit. The brushless DC motor structure and motor drive circuit are analyzed. The rotor is a permanent magnet structure while the stator is an armature winding. Usually, the three bridge arms of a three-phase bridge inverter composed of six high-power switching devices. When the winding is connected by Y solution, two of the six states have windings connected in series. For the feedback system, it is divided by sensored and sensorless frames. Sensored feedback system uses a position sensor, such as Hall sensor, while sensorless frame utilizes Back EMFs to determine the rotor position. Mathematical model is introduced next, including voltage equation, back EMFs, electromagnetic torque and equation of motion.

In the chapter 2, the requirements of motor controller design are analyzed. It is mentioned from main control state structure to open loop and close loop frames. The primary control logic is shown in Fig. 2.1. The design and experiment should have two stages of testing from open loop to close loop structures. To ensure the safe operation of the brushless DC motor system, Self-test and early warning function are designed to avoid system works in an uncertain state.

In the chapter 3, the entire hardware architecture and PCB board are built as shown in Fig. 3.10 and Fig. 3.11. The microcontroller is STM32F107VC, according to it has a wide range of timers, motor drive interface and communication interfaces. The BLDC motor is a common motor with 24V operating voltage, 9A current and hall sensor. Motor driver utilizes a high performance DRV8332 chip. Besides, the three stage power supplies are designed and the highspeed precision current sense amplifiers LT1999 are used to detect current values. The whole structure is built on a 50mm × 50mm compact board for reduce the space required for assembly.

In the chapter 4, the program is developed followed by the drive requirements of DRV8332, including the main function, communication control with PWM signals generation and warning interrupt. Two mainstream tools are used: Keil MDK and STM32CubeMX.

In the chapter 5, the performance of device is proved. The PWM generation of microcontroller, output voltage of DRV8332 and the motor speed are all in a relative stable and reliable state.

From the previous parts, all introduced tasks are achieved. Other than this, there have been many failed cases in the experiment and they are concluded. In APPENDIX 1, there is a fault detection of Hall sensor caused it works without pull-up resistors. In APPENDIX 2, a wrong signal launch sequence breaks the DRV8332. The APPENDIX 3 discusses the importance of using deadtime insertion. And the APPENDIX 4 mentions a fault caused by a wrong power on/off sequence. All these experiences could help others when they are in the same cases.

7.2   Future work

The current research progress is not very complete with some drawbacks. Therefore, several parts can be improved.

In the hardware design, the current detection due to electromagnetic interference has huge fluctuations and cannot be used. This can be improved by adding a shield layer to the PCB board. In addition, the heat dissipation of the chip is also very serious, and it is necessary to optimise the layout of the PCB.

For the software part, more control and filtering algorithms can be added to improve the performance of the drive and make the motor run more smoothly. At the same time, modern and popular communication interfaces with better compatibility can be considered for the enhancement.

LIST OF REFERENCES

[1] Antonio Franchi, Anthony Mallet. Adaptive Closed-loop Speed Control of BLDC Motors with Applications to Multi-rotor Aerial Vehicles. IEEE International Conference on Robotics and Automation, May 2017, Singapour, hal-01476812;

[2] Yan Zhuoa, Han Xiaoweia, Dai Xinxiaoa, Design and Implement of Welding Motor Control System Based on Wireless sensor network, Procedia Engineering, Volume 23, 2011, Pages 367-373, ISSN 1877-7058;

[3] Kamal Chakkarapani, Thyagarajan Thangavelu, Kalpana Dharmalingam, Pragadheeshwaran Thandavarayan, Multiobjective design optimization and analysis of magnetic flux distribution for slotless permanent magnet brushless DC motor using evolutionary algorithms, Journal of Magnetism and Magnetic Materials, Volume 476, 2019, Pages 524-537, ISSN 0304-8853;

[4] Shyi-Min Lu, A review of high-efficiency motors: Specification, policy, and technology, Renewable and Sustainable Energy Reviews, Volume 59, 2016, Pages 1-12, ISSN 1364-0321;

[5] Tze-Yee Ho, Yuan-Joan Chen, Po-Hung Chen, The design and implementation of a motor drive for foot rehabilitation, Computers & Electrical Engineering, Volume 56, 2016, Pages 795-806, ISSN 0045-7906;

[6] B. Abdi, M.M. Teymoori, H. Gholamrezaei, A.A. Nasiri,A Simple Analog BLDC Drive Control for Electro-Mechanical Energy Storage System, Energy Procedia, Volume 12, 2011, Pages 1002-1007, ISSN 1876-6102;

[7] E. Lee, "A micro HTS renewable energy/attitude control system for micro/nano satellites", IEEE Transaction on Applied Superconductivity, VOL. 13, NO. 2, JUNE 2003;

[8] T.J.E. Miller, Brushless permanent magnet and reluctance motor drive, Clarendon Press, Oxford, 1989;

[9] Bhim Singh, B.P.Singh, K Jain, Implementationof DSP based digital speed controller for permanent magnet brushless dc motor, Journal-EL,2003, 84:16-21;

[10] B. K. Lee ,M. Ehsani, Advanced BLDC motor drive for low cost and high performance propulsion system in electric and hybrid vehicles, IEEE electric machines and drives conference .2001,p.246-251;

[11] T.G. Wilson, P.H. Trickey, "D.C. Machine. With Solid State Commutation", AIEE paper I. CP62-1372, October 7, 1962;

[12] de Silva, Clarence W. Modeling and Control of Engineering Systems. CRC Press(2009). pp. 632–633. ISBN 1420076876.

[13] Xia, Chang-liang. Permanent Magnet Brushless DC Motor Drives and Controls. John Wiley and Sons(2012). pp. 18–19. ISBN 1118188365.

[14] Moczala, Helmut (1998). Small Electric Motors. London: Institution of Electrical Engineers. pp. 165–166. ISBN 085296921X.

[15] R.Krishnan, Permanent Magnet Synchronous and Brushless DC Motor Drive, Taylor & Francis Group, 2010;

[16] Danupon Kumpanya, Sattarpoom Thaiparnat, Deacha Puangdownreong, Parameter Identification of BLDC Motor Model Via Metaheuristic Optimization Techniques, Procedia Manufacturing, Volume 4, 2015, Pages 322-327, ISSN 2351-9789;

[17] Jian Sun, Yi Chai, Chunxiao Su, Zhiqin Zhu, Xianke Luo, BLDC motor speed control system fault diagnosis based on LRGF neural network and adaptive lifting scheme, Applied Soft Computing, Volume 14, Part C, 2014, Pages 609-622, ISSN 1568-4946;

[18] Mohd Tariq, T.K. Bhattacharya, Nidhi Varshney, Dhilsha Rajapan, Fast response Antiwindup PI speed controller of Brushless DC motor drive: Modeling, simulation and implementation on DSP, Journal of Electrical Systems and Information Technology, Volume 3, Issue 1, 2016, Pages 1-13, ISSN 2314-7172;

[19] Jordi-Roger Riba, Carlos López-Torres, Luís Romeral, Antoni Garcia, Rare-earth-free propulsion motors for electric vehicles: A technology review, Renewable and Sustainable Energy Reviews, Volume 57, 2016, Pages 367-379, ISSN 1364-0321;

[20] Jiahao Kou, A Study of Sensorless Commutation Methods for Brushless DC Motors, Department of Electrical and Computer Engineering University of Alberta, Master of Science, 2017, Pages 24-24;

[21] STM32F101xx, STM32F102xx, STM32F103xx, and STM32F105xx/ STM32F107xx datasheets, STMicroelectronics, 2018, http://www.st.com;

[22] STM32F10xxx Cortex-M3 programming manual (PM0056), STMicroelectronics, 2018, http://www.st.com;

[23] STM32F101xx, STM32F102xx, STM32F103xx, STM32F105xx/ STM32F107xx advanced Arm -based 32-bit MCUs reference manual, STMicroelectronics, 2018, http://www.st.com;

[24] DRV83x2 Three-Phase PWM Motor Driver datasheet, Texas Instruments, 2014, http://www.ti.com;

[25] Three Phase PWM Motor Driver, Texas Instruments, 2014, http://www.ti.com;

[26] MC7800 1.0 A Positive Voltage Regulators datasheet, ON Semiconductor, 2014, http://onsemi.com;

[27] LT1999-10/LT1999-20/LT1999-50 High Voltage, Bidirectional Current Sense Amplifier datasheet, Linear Technology, https://www.analog.com/en/products/lt1999.html

[28] Best Practices for Board Layout of Motor Drivers Application Report, Texas Instruments, Motor Drive Business Unit, SLVA959, November 2018;

[29] µVision User's Guide, ARM Keil, http://www.keil.com/support/man/docs/uv4/;

[30] Getting Started with MDK Create Applications with µVision® for ARM® Cortex®-M Microcontrollers, ARM Keil, https://www2.keil.com/mdk5/docs;

[31] Description of STM32F1 HAL and Low-layer drivers user manual (UM1850), STMicroelectronics, 2017, http://www.st.com;

[32] STM32CubeMX for STM32 configuration and initialization C code generation user manual (UM1718), STMicroelectronics, 2018, http://www.st.com;

APPENDIX 1: HALL SENSORS REQUIRE INDEPENDENT 5V SUPPLY AND REQUIRE PULL-UP RESISTERS

The Hall switch is an active magnetoelectric conversion device that converts a magnetic input signal into an electrical signal based on the Hall effect principle. It can be understood as a "magnetic switch." The non-contact trigger of the Hall switch has great advantages for product integration.

Common Hall sensors have the following three types:

- Unipolar Hall switch
- Bipolar Hall switch
- Omnipolar Hall switch

A unipolar Hall switch outputs a low-level signal when a magnetic pole approaches it and a high-level signal when the magnetic pole leaves. However, a unipolar Hall switch will specify a fixed magnetic pole (N pole/S pole) sensing.

Bipolar Hall switches typically have a latch function. When the pole exits, the Hall output signal does not change until another pole is sensed. In this type of brushless DC motor, this type of Hall switch is used to form a code sequence to detect the position of the rotator.

The omnipolar Hall switch does not specify a magnetic pole, and any magnetic pole is close to the output low level signal, leaving the output high level signal.The use of the Hall switch usually requires a pull-up resistor at the output, otherwise an output signal will appear as shown in the figure 36.

Figure 36. Hall signals detection without pull-up resistor

The STM32 family of micro-controllers is designed with a dedicated Hall signal interface, so no additional pull-up resistors are required in the circuit design.

# APPENDIX 2: COMPONENT FAILURE OR DAMAGE CAUSED BY A WRONG SIGNAL LAUNCHING SEQUENCE

The DRV8332 suffered multiple breakdown damage during the experiment. One of the factors is due to the wrong output switching sequence. The figure 37 is a weak voltage dynamic output test for PWM and RESET of one phase from STM32F107.
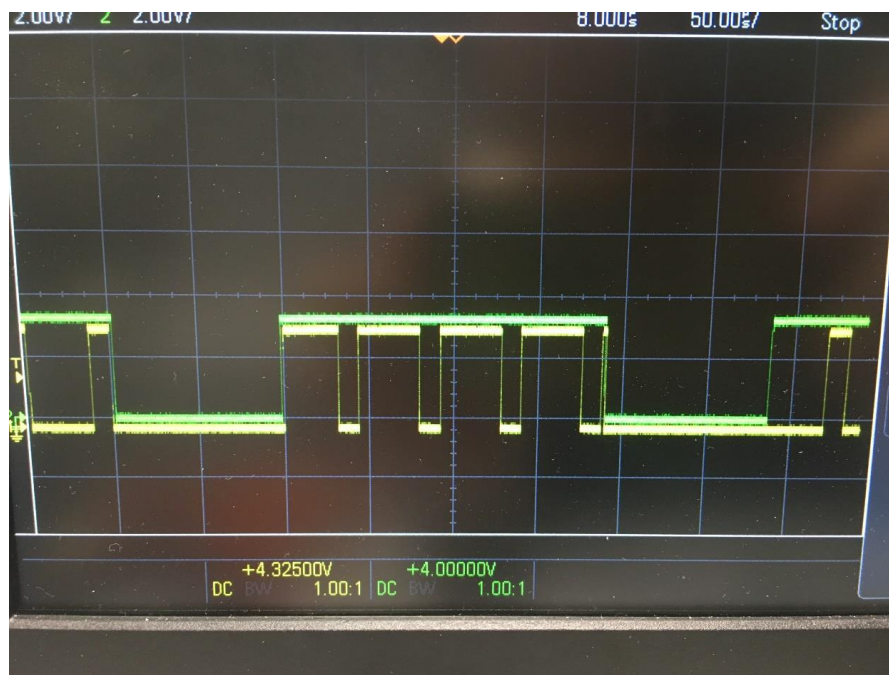

Figure 37. The voltage dynamic output test for PWM and RESET of one phase.

The green line represents the RESET output and the yellow line with more compact signals is the PWM output. It is hard to recognize the switching sequence even the time unit is 50μs. If we adjust the scale to 500ns as shown in Fig. Ⅱ.1. the switching sequence is clearer. This figure shows that when a new step is coming, the PWM output sets as low-level later than RESET output. If this combination uses on DRV8332, a fault OUT_X signal can be generated.

Since we first disabled the RESET port but also retained the PWM output, there is still current input in the phase that should be turned off. This causes the MOSFETs inside the chip breakdown due to excessive energy accumulation, as shown in figure 38 and figure 39. Therefore, in the design process, the order of signal output should be respect.
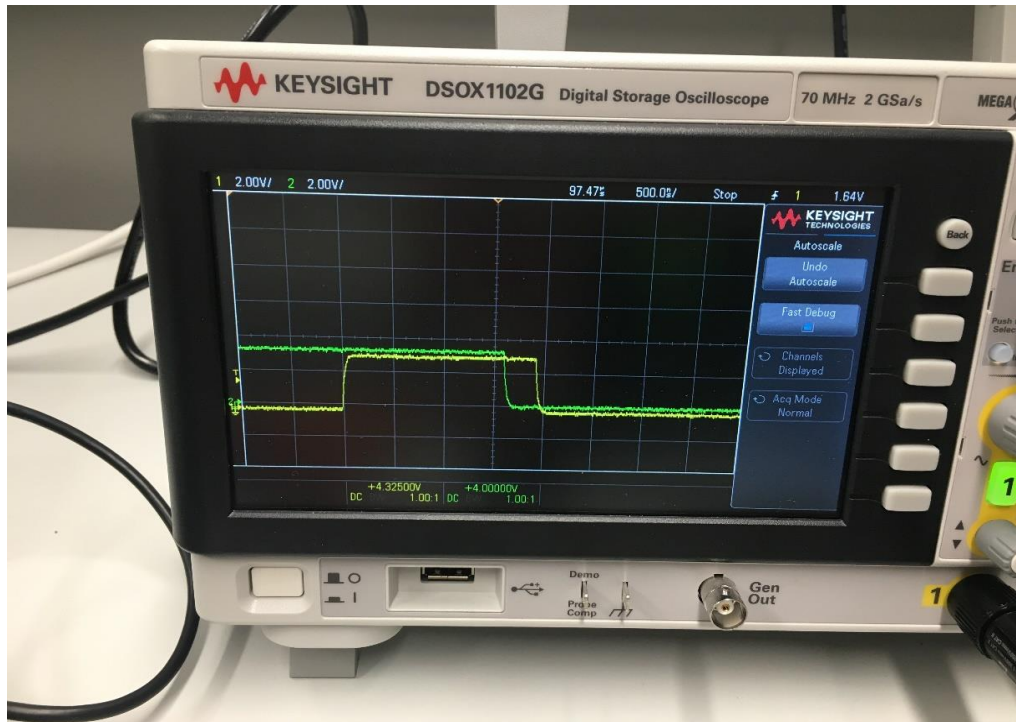
Figure 38. The voltage dynamic output edge test for PWM and RESET signals of STM32F107.
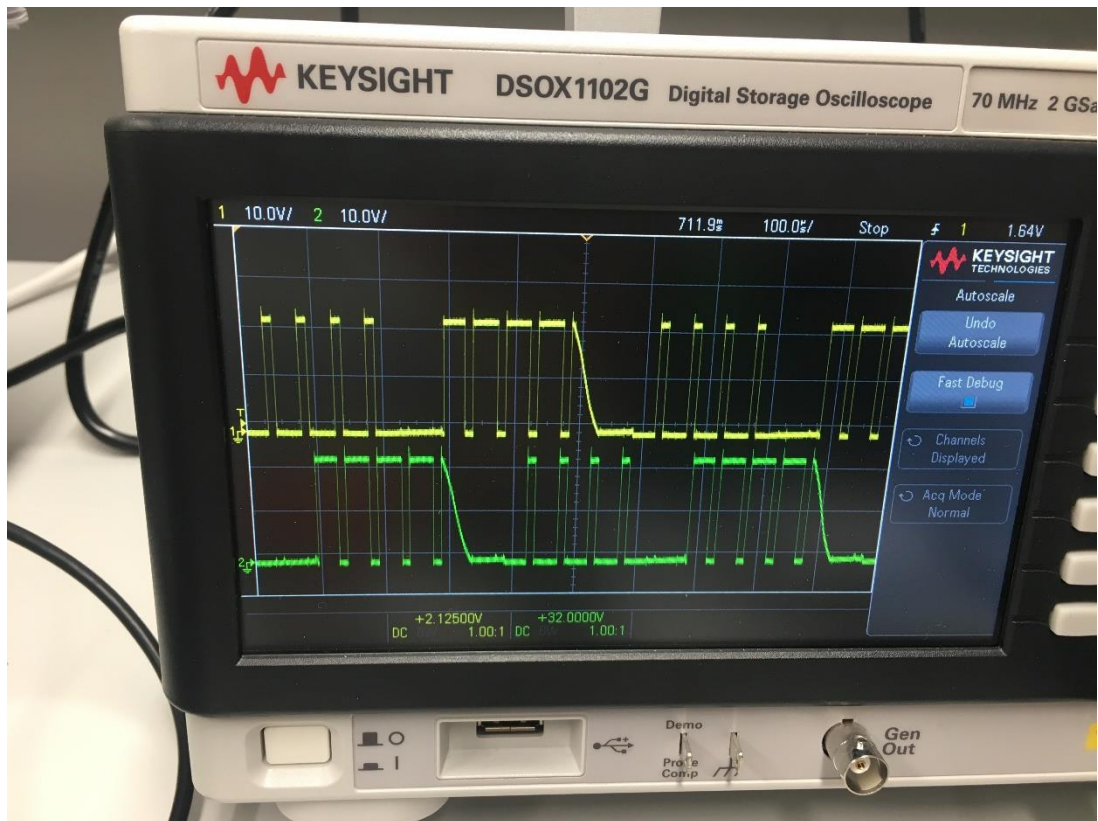
Figure 39. The fault OUT_A and OUT_B signals of DRV8332.

APPENDIX 3:THE IMPORTANCE OF DEADTIME INSERTION

Generally, high-power motors, inverters, etc., use H-bridges or 3-phase bridges composed of components such as high-power tubes and IGBTs. The upper half bridge and the lower half bridge of each bridge can never be turned on at the same time. But when the high-speed PWM drive signal reaches the control pole of the power component, the delay effect is often caused by various reasons. A half-bridge component does not turn off when it should be turned off, causing the power component to burn out. This effect, even for short a period causes large current spikes, which can increase thermal output, and when switching a few thousand times a second quickly wears out the MOSFETs.

The deadtime insertion (DTI) is after the upper half of the bridge is turned off, after delaying for a period to open the lower half of the bridge or after the lower half of the bridge is turned off, delay the opening of the upper half of the bridge for a period, thereby avoiding the burning of power components, as shown in figure 40. This delay is the deadtime. There is a 200ns deadtime insertion used for each two operating PWM channel, according to the DRV8332 datasheet that the propagation delay when FET is on/off is 38ns [24].

Figure 40. The PWM_A and PWM_B signals with a 200ns DTI.

APPENDIX 4: THE INFLUENCE OF POWER-ON STARTUP SEQUENCE

During the experiment of independent power supply, the regulated power supplies were used to output 24v, 12v and 5V power supplies and they were grounded. In one of the experiments, after the PWM output was turned off, then the 5V power supply of supporting controller turned off before 24V. At this point, the DRV8332 was burned instantly. After repeated recurrent experiments, the PWM outputs of the two channels are monitored at the moment of turning off the 5V power supply and got the result as shown in figure 41.
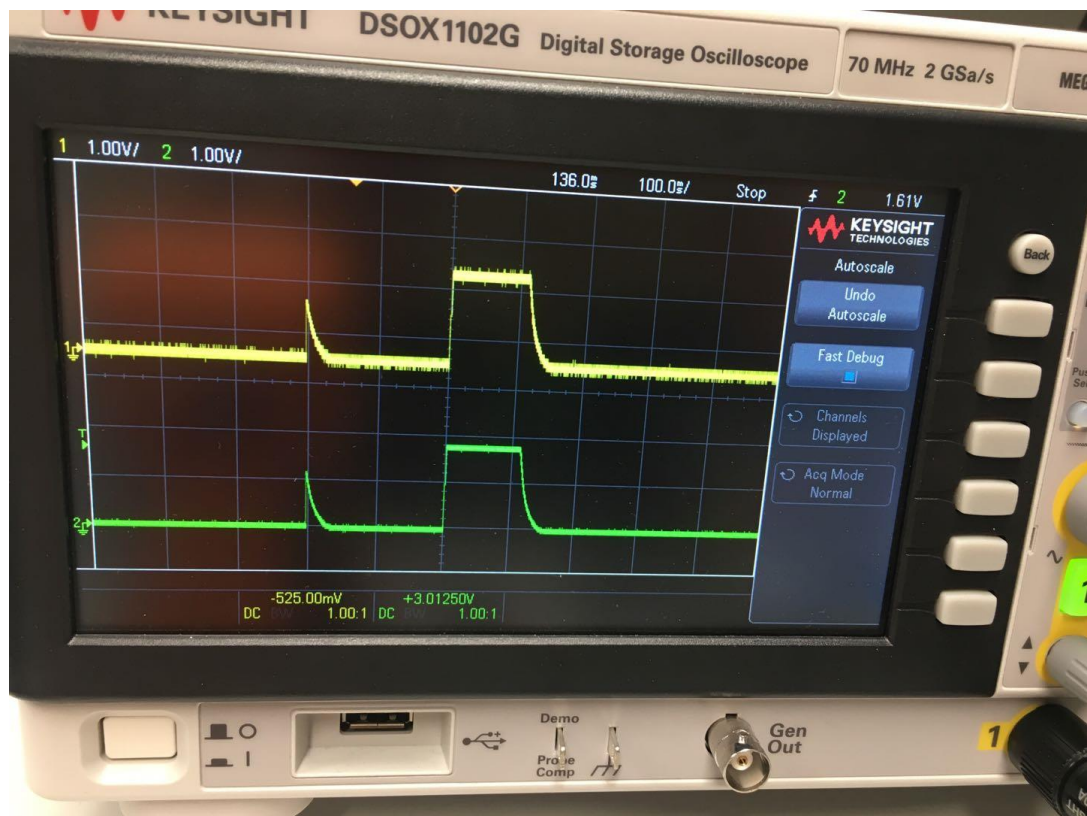
Figure 41. The output signals of PWM_A and RESET_A during shutdown 5V power.